UNIVERSITY OF OKLAHOMA

GRADUATE COLLEGE

MODELING AND CONTROL OF MICROGRID COMPONENTS

A DISSERTATION

SUBMITTED TO THE GRADUATE FACULTY

in partial fulfillment of the requirements for the

Degree of

DOCTOR OF PHILOSOPHY

By

ELHAM TAJIK
Norman, Oklahoma
2018

MODELING AND CONTROL OF MICROGRID COMPONENTS

A DISSERTATION APPROVED FOR THE
SCHOOL OF ELECTRICAL AND COMPUTER ENGINEERING

BY

Thordur Runolfsson, Chair

Nikola Petrov

Choon Yik Tang

John Jiang

Paul Moses

To my family.

Acknowledgements

Firstly, I would like to express my deepest appreciation and sincere gratitude to my academic advisor Professor Thordur Runolfsson for his continuous support of my PhD study and related research, for his patience, motivation, extensive knowledge and valuable advice. His care and guidance were sometimes all that kept me going.

My sincere thanks also goes to committee members, Professors Nikola Petrov, Choon Yik Tang, John Jiang and Paul Moses for serving as my committee members and for their valuable comments and suggestions.

My special thanks to Professor Joseph Havlicek for his support and for providing me an opportunity to work as part of Intelligent Transportation Lab (ITS).

I would like to thank my friends. My heartfelt thanks goes to Zeinab and Mahdi who have always been a major source of support.

A special thanks to my family. To my parents and my brother Ali and sister Elaheh that are always a source of energy and happiness for me. Last but not the least, I am deeply thankful to my husband Mohammadreza for supporting and encouraging me unconditionally.

Thank you very much, everyone! I will be grateful forever for your love.

Table of Contents

Acknowledgements **iv**

List of Figures **vii**

Abstract **ix**

Chapter 1. Introduction **1**
1.1 Background and Motivation 2
1.2 Literature Review 3

Chapter 2. Overview of modern power system challenges **10**
2.1 Modern Power Systems 10
2.2 Renewable Energy Sources (RESs) 11
2.3 Microgrid 12
2.4 Power System Control Architecture 15
2.4.1 Energy Management Control 16
2.4.2 DG Control 17
2.5 Summary 18

Chapter 3. Port-Hamiltonian Systems **20**
3.1 Passive Systems 20
3.2 Port-Hamiltonian System 21
3.2.1 Park-Transformation 24
3.2.2 Stability in Sense of Lyapunov Theory 26
3.3 Singular Perturbation Theory 27
3.4 Control of Port-Hamiltonian Systems 29
3.4.1 Interconnection and Damping Assignment (IDA) Control 30

Chapter 4. Port-Hamiltonian Systems and Power System Modeling **33**
4.1 Port-Hamiltonian Systems' Application in Power System Modeling . . . 33
4.2 Load Models . . . 44
4.2.1 Constant Impedance Load . . . 44
4.2.2 Induction Motor Load . . . 45
4.2.3 Constant Power Load . . . 47
4.3 Passivity of inductive loads and network . . . 53
4.3.1 Incremental system of inductive load and network . . . 53
4.4 Generator Control . . . 55
4.5 Summary . . . 60

Chapter 5. Modeling and Control of Inverter-based Generators **61**
5.1 Droop Control . . . 63
5.2 Virtual Synchronous Machines . . . 65
5.2.1 Average Modeling . . . 67
5.3 Proposed Technique for Modeling and Control of Inverter-based Generator 68
5.3.1 Generator Model For Current Source Inverter (CSI) . . . 70
5.3.2 Generator Model For Voltage Source Inverter (VSI) . . . 72
5.4 Dynamics and Stability of Interconnected Power System Components . 75
5.5 Control Design . . . 77
5.6 Stability . . . 82
5.7 Example . . . 85
5.8 Summary . . . 91

Chapter 6. Conclusion **92**

Bibliography **93**

List of Figures

2.1 A typical Microgrid schematic structure [26]. (Copyright 2008, IEEE) 13
2.2 DC-AC voltage conversion by an inverter [21]. (Reprinted with permission) . . . 15
2.3 Block Representation of DG units in connection to the grid [26]. (Copyright 2008, IEEE) . . . 18

4.1 The π line model. . . . 35
4.2 The T line model. . . . 37
4.3 Electrical Circuit of Three-phase Electrostatic Generator. . . . 43
4.4 The inductive load model. . . . 45
4.5 Constant power load. . . . 49
4.6 Block diagram of the proposed CPL model. . . . 51
4.7 The active power of CPL when there is a 20% drop in its terminal voltage. . . . 51
4.8 A 20% drop in terminal voltage of the modeled CPL. . . . 52
4.9 The reactive power of the modeled CPL for different values of α. . 52

5.1 A typical 2-level 3-phase structure of inverter-based generator in a microgrid [25]. (Copyright 2014, IEEE) . . . 68
5.2 SVM diagram of 2-level 3-phase Voltage Source Inverter [30]. (Copyright 2017, IEEE) . . . 69
5.3 V_{ref} is transformed into on/off signals for switches by a triangular wave (T_s is the switching period.) [30]. (Copyright 2017, IEEE) . 69
5.4 Schematic diagram of the open loop inverter-based generator design. 73
5.5 The proposed voltage source inverter-based controller. . . . 76
5.6 The open loop system consisting of a Current Source Inverter (CSI), a line and a load, all modeled as port-Hamiltonian systems. . . . 80
5.7 Schematic diagram of the closed-loop inverter-based controller. . . . 86
5.8 $\Delta\theta$ in open loop system for initial value $\frac{\pi}{6}$ . . . 86
5.9 $\Delta\theta$ for different values of α in the closed-loop system ($\alpha = 10^6$). . . 87
5.10 $\Delta\omega$ for different values of α in the closed-loop system ($\alpha = 10^6$). . . 87
5.11 Inverter-based generator terminal voltage for different values of α in the closed-loop system . . . 87

5.12 Generator and load terminal voltage. 88
5.13 $\tilde{u}_f$ when a 50 percent increase in load resistance occurs($\alpha = 10^6$). . 88
5.14 $\tilde{u}_p$ when a 50 percent increase in load resistance occurs($\alpha = 10^6$). . 88
5.15 Inverter-based generator terminal voltage when a 50 percent increase in load resistance occurs($\alpha = 10^6$). 89
5.16 Phase angle when a 50 percent increase in load resistance occurs($\alpha = 10^6$). 89
5.17 Frequency deviation when a 50 percent increase in load resistance occurs($\alpha = 10^6$). 89
5.18 Active power when a 50 percent increase in load resistance occurs($\alpha = 10^6$). 90
5.19 Reactive power when a 50 percent increase in load resistance occurs($\alpha = 10^6$). 90

Abstract

MODELING AND CONTROL OF MICROGRID COMPONENTS

Elham Tajik, Ph.D.
The University of Oklahoma, 2018

Supervisor: Thordur Runolfsson

Due to the increase in the integration of renewable energy resources into electrical power systems, there are various challenges that modern power systems are facing. A lot of issues in this subject are discussed under the concept of microgrid and their operational and control concerns.

Power electronic interfaces (converters, inverters) are necessary for connecting generation units based on renewable energy resources to the power grid. Consequently, inverter control is a primary issue in operating microgrids. Fast dynamics of power electronic interfaces results in different operating concerns and strategies for inverter-based generation units as compared to large conventional synchronous generators. To provide simplicity in operating inverter-based generation units, there are various control strategies based on emulating the critical properties of a conventional synchronous generator such as inertia and damping. This dissertation designs a novel operational and control model for controlled power electronic loads and inverter-based generators inspired by synchronous generators' equations and stated in port-Hamiltonian systems' formulation. This inverter generator controller is added to the inverter switching controller to enable the generator to behave in

a manner similar to a synchronous generator. We develop a control methodology based on Interconnection and Damping Assignment Passivity Based Control (IDA-PBC) strategy for the proposed inverter-based generator dynamics. We prove the stability of the designed closed loop system and develop a simulation model for the projected control strategy that includes an example system consisting of a constant impedance load, a $\pi-$modeled line and an inverter-based generator. We also develop a generic port-Hamiltonian model for loads that allows through the appropriate selection of structure and controls the mimicking of the behavior of complex loads that are connected to the grid through controlled power electronic interfaces.

Chapter 1

Introduction

For decades remote communities have been supplied by electrical energy through small grids. Fossil fuel that traditionally has been the primary energy source for distributed electricity generating units is rapidly being replaced by renewable energy resources. The integration of renewable energy resources and smart loads into power systems brings out new operation and control issues.

The relatively new concept of microgrids includes various control and operational challenges that small grids face in integrating renewable enrgy resources into their electrical power generation plan.

Through protection devices and switches, dependent on the operational requirements and events, microgrids may function either connected to the main grid or in an islanded mode. From the control perspective, the main grid sees the microgrid as an element acting in response to the control signals.

Power electronic devices as the interface between renewable energy resources and the grid, cause a very different characteristics of generation units based renewable energy resources and conventional synchronous machines. The very fast dynamics of power electronic devices requires appropriate operation and control schemes.

1.1 Background and Motivation

Microgrids may include various generation technologies such as traditional synchronous generators, DC generating units like photovoltaics and fuel cells or variable frequency AC units like wind turbines.

A traditional synchronous generator operates as a voltage source with adjustable magnitude. An excitation control is normally applied for regulating the terminal voltage of a synchronous generator. Dependent on the generator impedance, load current distortion and generator structure cause generator voltage distortion [19].

The shaft torque determines the amount of real power generation in a conventional synchronous generator. Load sharing in steady state operation is performed by governor control design based on droop characteristics of the generator's prime mover. This governor design regulate frequency of the stator voltage.

Non traditional generators such as DC generating units and variable frequency AC units, are connected to the grid through inverters. An inverter-based generator may be operated as either a current or voltage source [3]. The control of inverter-based generator is very fast and can be considered as instantaneous compared to the rest of grid dynamics. A sinusoidal waveform at the grid frequency is the desired output of the inverter-based generator. A model for generating a suitable reference waveform for feeding the pulse generator control of the inverter is needed. The desired magnitude and frequency of the output waveform as well as power exchange regulation can be attained by the correct generation of the reference waveform.

From the control point of view, in the grid-connected mode a microgrid

perceives the common point as an infinite bus by the voltage and frequency determined by the main grid, thus the control signals are active and reactive power. A microgrid in islanded operation mode needs to balance its own demand and supply and its control schemes are designed to establish the voltage and frequency signals of the common point.

In the modern power system, such as microgrids, loads are no longer simple impedance and motor loads but include loads that are interfaced to the grid through power electronic interfaces. The loads may have built in controllers for achieving a constant power load or other similar characteristics. Modeling loads of this type requires new methods for load modeling. In this dissertation, we develop a model for constant power load in port-Hamiltonian formulation.

1.2 Literature Review

In [2] control of microgrids in three levels is discussed and the main trends in controlling microgrids are reviewed. For the control purposes and as interface of distributed generating units supplied by renewable energy resources with the grid, inverter-based generators are modeled as synchronous generators.

Inverter based generators may be operated in two different operational modes, i.e. grid connected and isolated. Therefore, for the purpose of design and control, inverters are usually modeled either to supply the desired values of active and reactive power while connected to the main grid, called PQ inverter modeling or the magnitude and frequency of voltage in the stand alone operational condition [3].

Stand alone operational strategy is applied when frequency regulation is

needed (e.g. droop control). In this case the inverter is required to supply a desired value of voltage and frequency. Under PQ strategy, inverter-based generators are modeled as a current-controlled voltage source. In this case, the inverter-based generator is modeled to supply the set point of active and reactive power calculated by power flows of the system.

In a network model of a microgrid with purely inductive lines, active power flows are mainly functions of frequency and reactive power flows are functions of voltage magnitudes. Active power droop control and reactive power droop control are proportional controllers for controlling frequency and voltage magnitude, respectively [51, 54].

Droop control technique is a decentralized proportional control based on power-speed characteristic of synchronous generators is widely used to direct active power sharing in power systems with large scale fossil fuel based conventional generation units. Droop control has been a common method for regulating active and reactive power in microgrids with inverter-based generation units. In a microgrid with several parallel-connected inverter-based generator units, voltage and frequency droop control is a popular method to control the share of power that is delivered by each unit [37, 54]. In an inductive system the active and reactive of each generation unit is

$$P = \frac{EVsin\delta}{X} \tag{1.1}$$

$$Q = \frac{EVcos\delta - V^2}{X} \tag{1.2}$$

where E is the inverter terminal voltage amplitude, V is the common bus voltage amplitude, δ is the power angle and X is the output reactance of the inverter. As we can see in (1.1Literature Reviewequation.1.2.1) and (1.2Literature

Reviewequation.1.2.2), a network model of a micro-grid with purely inductive lines i.e. $\delta \approx 0$, active power flows are mainly functions of frequency and reactive power flows are functions of voltage magnitudes. Active power droop control and reactive power droop control are proportional controllers for controlling frequency and voltage magnitude, respectively.

Active power droop control builds a relation between active power and frequency that is very similar to the swing equation of synchronous generators [23],

$$\Delta\dot{\omega} = -d\Delta\omega - k_P(P - P_d) \tag{1.3}$$

where $\Delta\omega = \omega - \omega_d$, d is a damping ratio and ω_d (typically $\omega_d = \omega_r$) and P_d are the desired values of frequency and active power, respectively. Reactive power droop control is a proportional controller that relates reactive power flows and voltage magnitudes [23],

$$\Delta\dot{V} = -d\Delta V - k_Q(Q - Q_d) \tag{1.4}$$

where $\Delta V = V - V_d$, V_d and Q_d are the desired values of voltage magnitude and reactive power, respectively. The gains k_p and k_Q should be selected to satisfy the operational criteria such as control loop bandwidth and stability [35]. In systems with considerable line resistance, the original droop control in (1.3Literature Reviewequation.1.2.3)-(1.4Literature Reviewequation.1.2.4) due to coupling between P and Q does not produce satisfactory results. Several modified droop control strategies have been suggested to address this issue [5], [36].

Virtual Synchronous Machines (VSM) control technique is based on emulating the essential properties of a conventional synchronous generator such as inertia and damping to provide simplicity in operating inverter-based generation units. The mathematical model of synchronous generators consists of two set of

equations that describe its mechanical (swing equation) and electrical (the stator and rotor winding equations) parts. The higher order model of synchronous generators is applied to calculate the reference values for either virtual stator current or voltage. From a functional perspective, VSM is a controller that is added to the inverter switching controller to enable it to behave as a synchronous generator [3]. The functions in controlling an inverter-based generator can be expressed in three tasks:

1 To feed the VSM algorithm with voltage/current and frequency measurements.

2 To perform VSM algorithm i.e. applying the mathematical equations that are emulating electrical and mechanical performance of a synchronous generator and calculate a reference voltage (current) for Current Source Inverter (CSI) (Voltage Source Inverter (VSI)) in real time.

3 Employing the calculated reference values for generating the proper pulses to modulate power electronic switching of the inverter.

Zhong and Weiss in [58] introduce the dynamics and operation of synchronverters based on synchronous generators dynamics and apply frequency- and voltage-drooping mechanisms to share active and reactive power among parallel connected synchronverters. The approach in [58] is based on the full synchronous generator model equations (see e.g. (4.10equation.4.1.10)-(4.11equation.4.1.11)). However, they make certain steady state simplifications for the electrical part of generator that result in voltage source model, i.e. an equation of the form (4.14equation.4.1.14) for the electrical part of the inverter model. The inertial

model for the frequency dynamics of the inverter model is a full dynamic model mimicking a synchronous generator rotational dynamics. Alsiraji and El-Shatshat in [3] call the control algorithms that emulates the properties of traditional synchronous machines, Virtual synchronous machine (VSM) and categorize these methods into high and low order models. The low-order VSM models are based on swing equation and similar to the conventional droop control [12].

Fig 2.2DC-AC voltage conversion by an inverter [21]. (Reprinted with permission)figure.2.2 illustrates a typical inverter-based distributed generation unit that consists of an energy source unit that converts renewable energy to DC form of electricity, a capacitor bank to stabilize the DC link voltage, an inverter that converts electricity to AC form with the network frequency and a filter to remove the high frequency contents.

These VSM techniques are basically divided in two categories:

- Current Source Inverter (CSI)- In this methods the grid voltage is measured and virtual synchronous machine algorithm calculates the reference current for the pulse generating unit [6, 8, 9].
- Voltage Source Inverter (VSI)- In this methods the pulse generating unit is fed by the reference voltage that is calculated using the measured phase currents [4, 48, 57, 58].

Hill in [20] proposes an approach for adding load dynamics to steady-state load behavior in order to emulate the dynamical response of loads to a step voltage change. He defines a nonlinear dynamical relationship between the desired active and reactive power of the load i.e. P_d and Q_d and the load voltage V as,

$$\dot{P}_d + f_P(P_d, V) = g_P(P_d, V)\dot{V} \tag{1.5}$$

and the similar equation for reactive power, i.e.

$$\dot{Q}_d + f_Q(Q_d, V) = g_Q(Q_d, V)\dot{V} \tag{1.6}$$

This can be more generalized as a higher order degree,

$$f_P(P_d^{(n)}, P_d^{(n-1)}, ..., \dot{P}_d, P_d, V^{(m)}, ..., \dot{V}, V) = 0 \tag{1.7}$$

$$f_Q(Q_d^{(n)}, Q_d^{(n-1)}, ..., \dot{Q}_d, Q_d, V^{(m)}, ..., \dot{V}, V) = 0$$

This model is shown to capture the dynamics of constant impedance load and motor load. A simpler representation of this model assumes an exponential recovery to the steady state value [20]. For active power,

$$T_p\dot{P}_d + P_d = f(V) + g(V)\dot{V} \tag{1.8}$$

where $f(V) = CV^{\alpha_P}$. The size of power overshoot in (1.8Literature Reviewequation.1.2.8) is determined by the negative index α_P.

Kundu and Hiskens in [31] discuss the effect of significant power quality events such as large scale voltage sags (more that 20%) on Plug-in Electrical Vehicle (PEV) charger loads that may be the loss of a large portion of the total loads. For a PEV charger load with unity power factor the load active power P, voltage V and the susceptance at the load bus b are modeled to be related as,

$$f(P, b, V; r, x, V_\infty) = \left((1 - bx)^2 + (br)^2\right) V^4 + (2Pr - V_\infty^2)V^2 + P^2(r^2 + x^2) = 0 \tag{1.9}$$

where r, V_∞ and x are model's parameters. Equation (1.9Literature Reviewequation.1.2.9) defines a complex steady state relationship between power and voltage that matches field data. This complex model could be made into a dynamic model using an approach similar to [20].

Allen and Ilic in [2] show that applying a static or slow dynamic model for PQ loads while including the transmission line dynamics results in instabilities around the desired load flow solution. A simple dynamic representation of CPLs can be found in [1, 2, 43],

$$\dot{g} = \frac{1}{\tau}\left[P_{ref} - \frac{|i_l|^2}{g}\right] \tag{1.10}$$

where P_{ref} is the constant real power that load is expected to consume, g is the conductance value of the load and its conductance matrix is as $G = gI$ and i_l is the load port current in $dq0$ coordinates. The PQ load model in [2] includes a dynamic susceptance part (B) for an admittance in the form $G + jB$ as well.

The CPL dynamics in (1.10Literature Reviewequation.1.2.10) for a relatively long time constant behaves as a constant impedance load. As is shown in [2] there is a critical value of τ for which the system obtain from the load (1.10Literature Reviewequation.1.2.10) connected to a transmission line becomes unstable. Consequently for short time constants, the CPL model in (1.10Literature Reviewequation.1.2.10) results in instabilities and therefore, this model is not a good representation of CPL dynamics where time constants are typically very small.

At the load input terminal, CPLs acts like a negative incremental impedance. For constant power of the load, the current and voltage at terminals,

$$|i_l| = \frac{P_{ref}}{|v_l|} \tag{1.11}$$

by (1.11Literature Reviewequation.1.2.11)the voltage drop causes increase in the current. Therefore, to study small signal stability, some papers apply a negative impedance model for CPLs. This equivalent impedance of CPLs may be used in impedance-based small signal stability analysis [7, 44, 45, 53].

Chapter 2

Overview of modern power system challenges

2.1 Modern Power Systems

A power system is a highly nonlinear, complex and large system whose main objective is to deliver electricity from generators to loads. Traditionally, electricity is generated in large generation plants and is transported to the loads by hierarchical structure of high, medium and low voltage networks while all these equipment and functions are protected by various protection schemes. Nowadays, introduction of new technologies has presented new challenges regarding operating and analyzing of modern power systems:

- *Renewable Energy Sources (RES):* Energy policies have been developed to encourage use of renewable energy resources as the primary form of energy. RES and their potential to decrease fossil fuels consumption and greenhouse gas emissions generates interest in integrating a large number of RES in electric power systems. The European Union has set a target of 27% for the share of renewable energy sources of EU's final energy consumption by 2030.

  Beside all the benefits of integrating renewable energy resources in power systems, their uncertain nature introduces operational challenges. Unlike traditional generation, due to their uncertainty, renewable energy based generation units can not be scheduled. The generated electricity is either in DC form or variable frequency with much larger bandwidth.

- *Fast responding generation units:* In a large conventional synchronous generator, the rotational part is the interface between the primary energy source and the grid. Slow mechanical dynamics due to large inertia and damping results in slower response in case of contingency event. Control and operation of conventional synchronous generators are based on time scale separation between mechanical and electrical parts. However, in renewable energy based generation units, because the interface between primary energy source and grid is provided by fast power electronics devices, there is no natural time scale separation, inertia or damping.

- *Controllable Loads:* New models for studying the performance of loads are needed. Traditional load models such as constant impedance load and motor load are no longer sufficient and improved models are needed to capture dynamics of modern power system in stability studies and their operation. Furthermore, loads may include generation so they are capable of delivering energy to the grid that results in two directional power flow.

- *Less reserve capacity:* Increasing demand results in highly stressed operation of power systems. Therefore, to insure reliability and security of the system new operational techniques are required.

2.2 Renewable Energy Sources (RESs)

A small individual generation or storage unit (less than 50-100 MW) that is located close to the load is called Distributed Generation (DG) [14]. According to the definition by the International Council on Large Electric Systems (CIGRE), generation units that are not centrally planned and dispatched and are sufficiently

smaller than central generation units are called DG [14].

There are several problems that are needed to be addressed in order to integrate renewable energy sources into power systems [39]:

- Scheduling and dispatching generation units based on renewable energy resources considering uncertainties in supply and demand.
- Economical operation of microgrids with high penetration of renewable energy resources in acceptable reliability.
- Providing proper demand side management scheme.
- Providing proper protection schemes which are capable of dealing with bidirectional power flows.
- Developing proper voltage and frequency control schemes to operate power electronic interfaces of renewable energy resources and grid.
- Developing proper market mechanisms.

2.3 Microgrid

For decades remote communities have been supplied electrical energy isolated from the main grids. Small grids with distributed electricity sources at the distribution level that contain sufficient generation to supply most or all of their demand are called Micro-grids. Historically, the source of energy for remote grids has mostly been fossil fuel. Nowadays, integrating RES into micro-grids is a priority and consequently the electrical power system is dramatically changing from centralized generation to distributed generation.

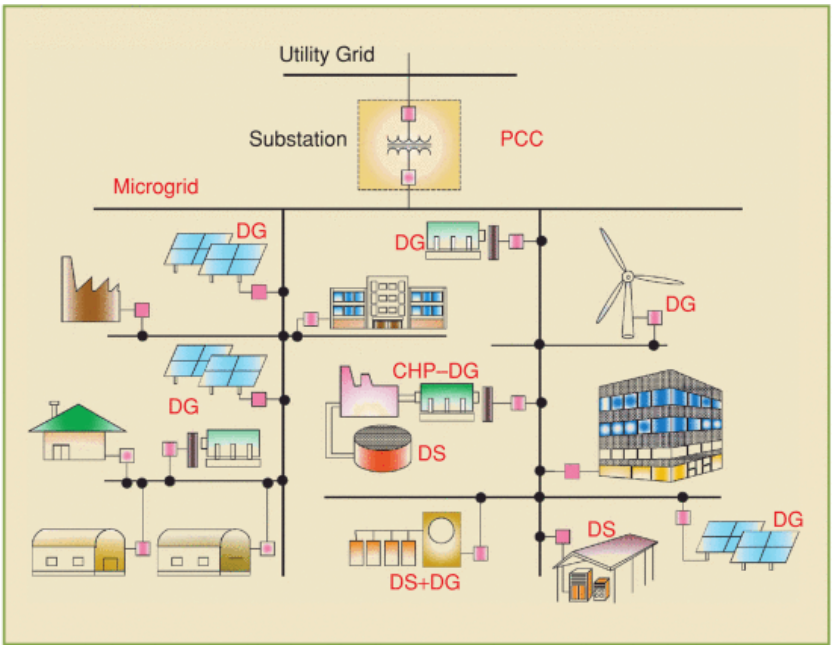

Figure 2.1: A typical Microgrid schematic structure [26]. (Copyright 2008, IEEE)

Fig 2.1A typical Microgrid schematic structure [26]. (Copyright 2008, IEEE)figure.2.1 shows a typical Microgrid schematic structure that is part of a distribution network that is connected to the rest of grid through Point of Common Coupling (PCC). Microgrid in normal operation works while connected to the grid in PCC so the voltage magnitude and phase at this point is enforced by the grid. However, mircogrids are capable of working in islanded mode in the event of a contingency occurrence that leads to accidental islanding or a scheduled disconnection from the main grid. Therefore, microgrid must be capable of providing sufficient power generation to deliver to local loads and be equipped by suitable control platform that insure the reliable and stable operation of it in stand alone operational mode.

Within a microgrid, electricity may be provided by two types of Distributed Generations (DGs). Conventional generation that are usually synchronous gener-

ators with rotating parts and inverter-based generation units. These two types of DGs require different control and operation schemes.

Due to uncertainty in renewable energy sources and single-phase loads, microgrids are subject to large changes. Renewable energy sources are noncontrollable and they are required to maintain an adequate power quality specified by Grid Code.

To enjoy economical and environmental benefits of higher penetration of renewable energy source in electric grids, developing reliable control techniques for operating these distributed power generation units is required. Electricity generated by RES is either at high variable frequency or DC, therefore it requires power electronics converters and inverters to get connected to the grid. For example, photovoltaic arrays generate DC voltage that requires inverter for being connected to the grid and wind-turbines generate variable frequency voltage that needs to be first converted to DC and then to the grid frequency by inverters. Thus, inverter-based generation is gaining ever-increasing interest and is increasingly integrated into electrical grids. Detailed modeling of power electronics components in a microgrid system that includes a large number of inverter-based generation units, results in increased computing time. Designing fast and at the same time complex enough techniques to adequately control power electronics circuits at the interface between the grid and the renewable energy source is vital for delivering high-quality power.

In traditional power generation units, large synchronous generators with slow dynamics that get connected to the grid are characterized by their large inertia and damping. In the event of a disturbance or fault in the grid, this static characteristics of traditional synchronous generators when combined with protection devices provides support for maintaining the stability of power system.

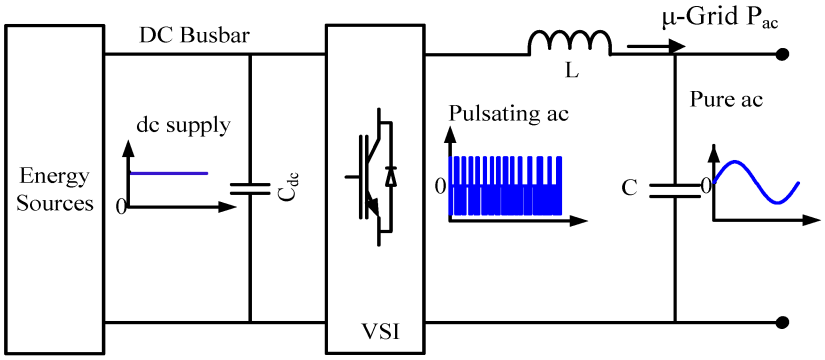

Figure 2.2: DC-AC voltage conversion by an inverter [21]. (Reprinted with permission)

.

Fast response of power electronic interface of renewable energy resources and grid, poses operational challenges to preserve stability.

Fig 2.2DC-AC voltage conversion by an inverter [21]. (Reprinted with permission)figure.2.2 illustrates a typical inverter-based distributed generation unit that consists of an energy source unit that converts renewable energy to DC form of electricity, a capacitor bank to reduce fluctuations and stabilizes the DC link voltage, an inverter that converts electricity to AC form at the network frequency and a filter to eliminate the high frequency content.

Inverters consist of semiconductor elements and a pulsing controller is necessary to generate the desired waveform of electricity [26]. By sequential turning on and off of transistors and diodes in the inverter, the input DC voltage is transformed to AC voltage in its output terminal. The triggering commands are usually generated in a Pulse Width Modulation (PWM) unit.

2.4 Power System Control Architecture

The appropriate operation and control scheme of an inverter-based generator depends on the type of microgrid loads and its mode of operation. Most published literature in microgrid control strategies present the control of microgrid problem as a hierarchical control in different levels [21]. A DG unit may be dispatchable and the supervisory control decides its desired amount of output power or nondispatchable and its output power is often determined by the optimal operational condition of its energy source [26].

2.4.1 Energy Management Control

In an electrical power system, a centralized control is responsible for economic dispatch and scheduling generation. This centralized Energy Management Control collects data, processes the gathered data and forecasts power need, calculates optimal dispatch/scheduling of generation units and as a supervisory control transmits control signals to plants.

The recent approach in microgrid supervisory control is consensus-based control instead of the centralized control. In consensus-based control these are two-way communications and transferring of data such as voltage and frequency measurements between each generator and controlled load and its neighbors.

A power and energy management strategy is required for a microgrid with more than a single generation unit. As a microgrid often has multiple small distributed generation units with different capacities and characteristics, and because of the fast response of its renewable energy based generation units, faster power

and energy management strategies compared to conventional power systems is essential for stable operation.

A real time energy management controller receives the current and forecasted data of market, generation and load and processes these information to generate control decisions such as power flows. Through energy and power management strategy active and reactive demand is shared among generation units by assigning the power set points and enables synchronizing the microgrid with the main grid.

While connected to the main grid each of the generation units of a microgrid supply the desired power and is controlled to act as a PQ or a PV bus and the main grid is responsible to the difference between the demand and local generation. In islanded operation, the total of demand must be met by the local generation or some of the less sensitive loads are shedded to achieve the generation-demand balance. Power and Energy management control is responsible to provide long-term energy balance to maintain sufficient reserve capacity by considering requirements and limitations such as cost, time dependancy and environmental effects of each generation unit and short-term power balance by providing acceptable dynamical response [26]. Through appropriate load shedding and power sharing among generation units, power balancing strategy enables local controllers to regulate voltage and frequency and restore and resynchronize the system in the event of a contingency.

2.4.2 DG Control

As shown in Fig 2.3Block Representation of DG units in connection to the grid [26]. (Copyright 2008, IEEE)figure.2.3 regarding to each DG unit in a microgrid, there is a primary source of energy, an interface between the energy source and the electrical part and a switch to connect it to the grid. In a conventional synchronous generator this interface is its rotor shaft. A governor controls synchronous generator speed and active power and an Automatic Voltage Regulator (AVR) controls voltage and reactive power. In the case of renewable energy resources, a power electronic circuit and its controller perform as interface to generate the desired AC electricity.

When a significant share of the the total generation is based on renewable energy sources, operating the grid is complex. To sustain stability and reject undesirable behaviors, it is beneficial to operate them in a manner that is similar to traditional synchronous generators. For this purpose, control techniques can be applied for operating inverter-based generators so that they mimic some crucial properties of bulky synchronous generators. This is a realistic way for integrating renewable energy sources in power grids while preserving stability and is based on applying control techniques that produce virtual inertia and damping by mimicking the behavior of synchronous generators.

2.5 Summary

Modern power systems that include RES, various types of DGs that are either conventional and rotatory units or inverter-based generators and controllable loads that enable demand side management strategies introduce new operational and analysis challenges. Microgrid concept as a single controllable system that is a

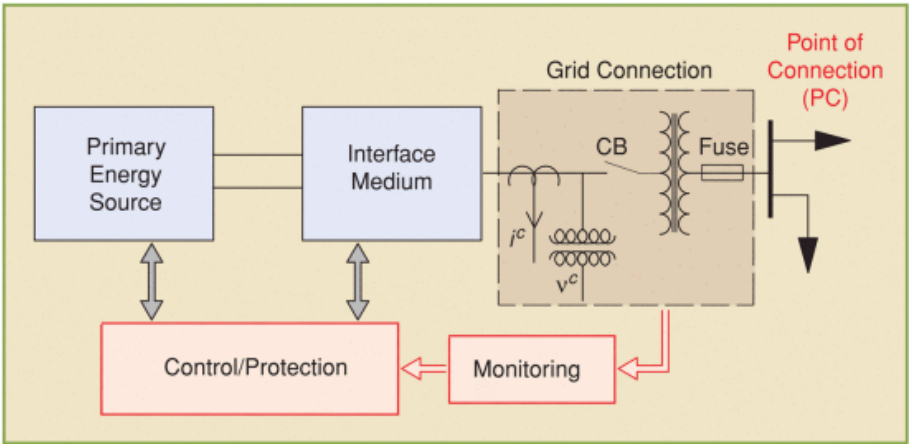

Figure 2.3: Block Representation of DG units in connection to the grid [26]. (Copyright 2008, IEEE)

cluster of loads and smaller size generation units and provides its local power demand are reviewed in [32, 33, 39] to provide reliable integration of DGs and controllable loads into power systems.

The control of a microgrid at different levels and each level in the control hierarchy is in a different time scale. In this dissertation we focus on the following two problem:

1 Primary control of inverter-based generators that may be the power generating units of a microgrid.

2 Framework for modeling and control of complex loads that cannot be modeled by conventional load modeling methods.

Chapter 3

Port-Hamiltonian Systems

3.1 Passive Systems

Consider a non-linear system in the form [49]

$$\dot{x} = a(x) + b(x)u \tag{3.1}$$

$$y = c(x)$$

where $u, y \in \mathbb{R}^m$ are input and output port variables of the system and $x \in \mathbb{R}^n$ is the system state. This system is passive if there exists an energy function $H : \mathbb{R}^n \to \mathbb{R}$ with $H(x) \geq 0$ for every x, such that

$$H(x(t)) - H(x(0)) \leq \int_0^t u^T(\tau)y(\tau)d\tau \tag{3.2}$$

for all inputs and initial conditions and for all t.

This passive system satisfies the energy-balance equation in the form

$$H(x(t)) - H(x(0)) = \int_0^t u^T(\tau)y(\tau)d\tau - d(t) \tag{3.3}$$

where $d(t) \geq 0$ is called the dissipation function. From (3.3Passive Systemsequation.3.1.3) we can conclude

- For an unforced system, i.e. $u = 0$, $H(x(t)) = H(x(0)) - d(t)$, thus, $H(x(t)) \leq H(x(0))$ that means that the energy function is nonincreasing and in presence of energy dissipative components in the system, it is decreasing.

- If the energy get extracted from the system by some input such as $u = -Ky$ where $K = K^T > 0$ then

$$H(x(t1)) - H(x(0)) = -\int_0^t y^T(\tau)Ky(\tau)d\tau - d(t) < -d(t) \tag{3.4}$$

that means the energy decreases with a higher rate.

- A bounded amount of energy can be extracted from the system [56].

$$H(x(0)) \geq -\int_0^t u^T(\tau)y(\tau)d\tau + d(t) \geq -\int_0^t u^T(\tau)y(\tau)d\tau \tag{3.5}$$

Proposition 3.1.1. [55], page 39. If $H(x)$ is differentiable, passivity of the system (3.1Passive Systemsequation.3.1.1) means

$$\nabla_x H^T(x)a(x) \leq 0 \tag{3.6}$$

and

$$c(x) = b^T(x)\nabla_x H(x) \tag{3.7}$$

If $H(x^*) = 0$ where x^* is the equilibrium state and $H(x) > 0$ for $x \neq x^*$ and $d(t) \neq 0$ then (3.1Passive Systemsequation.3.1.1) is asymptotically stable at $x = x^*$. For lossless system i.e. $d(t) = 0$, (3.1Passive Systemsequation.3.1.1) at $x = x^*$ is stable but not asymptotically stable.

3.2 Port-Hamiltonian System

Dynamical systems may be perceived as devices to transform energy. In this case, to study its behavior, a complex, nonlinear, multi-physics dynamical system can be decomposed into simpler energy transforming subsystems interconnected by ports. Adjusting the behavior of the system can be achieved by manipulating the overall energy of the system through adding another dynamical system to the main plant

as the control process and using the interconnections. Due to the fact that energy is a fundamental physical concept, this modeling scheme is applicable in various types of energy such as electrical, mechanical, thermal and so on.

A physical system can be described by a power preserving interconnected set of energy storing elements, energy dissipating elements and ports to interact with other systems.

A specific form of energy systems is the so-called port-Hamiltonian formulation that provides a general way for modeling, analysis and control of dynamical systems. Port-Hamiltonian formulation is an effective and systematic method to model, analyze and control advanced power systems [47], [15]. In this formulation, a Hamiltonian function is defined for each subsystem of the overall system and the subsystems are interconnected by input/output ports that transfer power. A general port-Hamiltonian system has the form,

$$\begin{aligned} \dot{x} &= (J(x) - R(x))\nabla H(x) + g(x)u \\ y &= g^T(x)\nabla H(x) \end{aligned} \tag{3.8}$$

where $H : \mathbb{R}^n \to \mathbb{R}$ is the Hamiltonian function, $J(x)$ is the interconnection matrix, $R(x)$ is the dissipation matrix and $x \in \mathbb{R}^n$. The interconnection and dissipation matrices satisfy the following conditions, $J(x) = -J^T(x)$, $R(x) = R^T(x)$ and $R(x) \geq 0$. $u \in \mathbb{R}^m$ and $y \in \mathbb{R}^m$ are the input and output port variables. The input and output variables are conjugated and their product is power. The Hamiltonian function is often the stored energy of the system and the term $\nabla H(x)$ is its gradient with respect to state variables of the system. The time derivative of the Hamiltonian function is,

$$\dot{H}(x) = \nabla H^T(x)\dot{x} = -\nabla H^T(x)R(x)\nabla H(x) + y^T u = P_D + P_T \tag{3.9}$$

where P_D is the dissipated power and P_T is the exchanged power via the input-output port, $y^T u = P_T$. Therefore, we can say the rate of change in the stored energy equals the sum of the total power exchanged through input-output ports and the dissipated power in the system. In electrical systems, currents and voltages are the signals at input/output ports and in mechanical systems input/output ports' signals are forces/torques and velocities/frequency.

Many physical systems can be described in port-Hamiltonian framework. When modeling a complex system, each element is viewed as a device to transfer energy and can be presented in port-Hamiltonian formulation and then connected to the other elements by its input-output ports. The total port-Hamiltonian model has a Hamiltonian function that is equal to sum of the Hamiltonian functions of all individual components.

Example 3.2.1. Two Port-Hamiltonian system's interconnection

Consider two port-Hamiltonian systems described by,

$$\dot{x}_1 = (J_1(x_1) - R_1(x_1))\nabla H_1(x_1) + g_1(x_1)u_1 + e_1(x_1)v_1 \tag{3.10}$$

$$y_1 = g_1(x_1)^T \nabla H_1(x_1)$$

and

$$\dot{x}_2 = (J_2(x_2) - R_2(x_2))\nabla H_2(x_2) + g_2(x_2)u_2 + e_2(x_2)v_2 \tag{3.11}$$

$$y_2 = g_2(x_2)^T \nabla H_2(x_2)$$

where u_1 and u_2 are input ports and v_1 and v_2 are the control or disturbance inputs. With the interconnection law $y_1 = u_2$ and $u_1 = -y_2$ the overall Hamiltonian function is $H(x_1, x_2) = H_1(x_1) + H_2(x_2)$ and $\nabla H(x_1, x_2) = \begin{bmatrix} \nabla H_1(x_1) \\ \nabla H_2(x_2) \end{bmatrix}$. The

Hamiltonian representation of the overall system is,

$$\begin{bmatrix}\dot{x}_1\\ \dot{x}_2\end{bmatrix} = (J(x_1,x_2) - R(x_1,x_2))\nabla H(x_1,x_2) + E(x_1,x_2)v \tag{3.12}$$

where,

$$J(x_1,x_2) = \begin{bmatrix} J_1(x_1) & -g_1(x_1)g_2(x_2)^T \\ g_2(x_2)g_1(x_2) & J_2(x_2)\end{bmatrix}$$

$$v = \begin{bmatrix}v_1\\ v_2\end{bmatrix},\ R(x_1,x_2) = \begin{bmatrix}R(x_1) & 0\\ 0 & R(x_2)\end{bmatrix},\ E(x_1,x_2) = \begin{bmatrix}e_1(x_1) & 0\\ 0 & e_2(x_2)\end{bmatrix}.$$

3.2.1 Park-Transformation

Signals in a balanced three phase power system in steady state have the form,

$$x = \begin{bmatrix} Xcos(\theta(t)) & Xcos(\theta(t) - \frac{2\pi}{3}) & Xcos(\theta(t) - \frac{4\pi}{3})\end{bmatrix}^T \tag{3.13}$$

where $\theta(t) = \theta_r(t) + \theta_0 = \omega_r t + \theta_0$ and ω_r is the nominal frequency. The Park-transformation [18] maps the 3-phase network dynamical equations into a rotating framework. Let $T(\theta_r)$ be the Park-transformation matrix [18],

$$T(\theta_r) = \sqrt{\frac{2}{3}}\begin{bmatrix} cos(\omega_r t) & cos(\omega_r t - \frac{2\pi}{3}) & cos(\omega_r t - \frac{4\pi}{3}) \\ sin(\omega_r t) & sin(\omega_r t - \frac{2\pi}{3}) & sin(\omega_r t - \frac{4\pi}{3}) \\ \frac{1}{\sqrt{2}} & \frac{1}{\sqrt{2}} & \frac{1}{\sqrt{2}}\end{bmatrix} \tag{3.14}$$

and let $\bar{x} = T(\theta_r)x$ be a transformed coordinate. Consider a linear system of the form,

$$\dot{x}(t) = Ax(t) + Bu(t) \tag{3.15}$$

$$y(t) = Cx(t) + Du(t)$$

where $A \in \mathbb{R}^{3\times3}$, $B \in \mathbb{R}^{3\times3}$, $C \in \mathbb{R}^{3\times3}$, $D \in \mathbb{R}^{3\times3}$

Proposition 3.2.1. Assume that A, B, C and D commute with $T(\theta_r)$. Then $\bar{x}(t) = T(\theta_r)x(t)$ satisfies the equation,

$$\dot{\bar{x}}(t) = (\omega_r N + A)\bar{x}(t) + B\bar{u}(t) \tag{3.16}$$

$$\bar{y}(t) = C\bar{x}(t) + D\bar{u}(t)$$

where $N = \begin{bmatrix} 0 & -1 & 0 \\ 1 & 0 & 0 \\ 0 & 0 & 0 \end{bmatrix}$ and $\bar{u}(t) = T(\theta_r)u(t)$ and $\bar{y}(t) = T(\theta_r)y(t)$ are the input and output ports in the rotating coordinates.

Proof - $T^T(\theta_r)T(\theta_r) = I$ and thus $T^{-1}(\theta_r) = T^T(\theta_r)$.

$$\dot{\bar{x}}(t) = \dot{T}(\theta_r)x(t) + T(\theta_r)\dot{x}(t)$$

$$= \dot{T}(\theta_r)T^T(\theta_r)T(\theta_r)x(t) + T(\theta_r)Ax(t) + T(\theta_r)Bu(t)$$

$$= (\dot{T}(\theta_r)T^T(\theta_r) + A)\bar{x}(t) + B\bar{u}(t)$$

and $T(\theta_r)y(t) = T(\theta_r)Cx(t) + T(\theta_r)Du(t)$. It is easy to see that,

$$T^T(\theta_r)\dot{T}(\theta_r) = \omega_r N$$

Thus,

$$\dot{\bar{x}} = (\omega_r N + A)\bar{x}(t) + B\bar{u}(t)$$

$$\bar{y}(t) = C\bar{x}(t) + D\bar{u}(t)$$

Remark 3.2.1. In the remainder of the dissertation we refer to the transformed coordinates as $dq0$ coordinates. Note that $T(\theta_r)$ is evaluated at the system frequency ω_r.

Remark 3.2.2. The matrix $T(\theta_r)$ is a unitary matrix, i.e. $T(\theta_r)T^T(\theta_r) = I$. Consequently, $\bar{y}^T(t)\bar{u}(t) = y^T(t)T^T(\theta_r)T(\theta_r)u(t) = y^T(t)u(t)$.

Remark 3.2.3. If the input to the system (3.15Park-Transformationequation.3.2.15) is a three phase steady state signal of the form (3.13Park-Transformationequation.3.2.13) then the input $\bar{u}(t)$ in (3.16equation.3.2.16) is constant $\bar{u}$. Consequently, the transformed system has constant steady state given by $(\omega_r N + A)\bar{x} + B\bar{u} = 0$ and the output has the constant value $\bar{y} = C\bar{x} + D\bar{u}$.

3.2.2 Stability in Sense of Lyapunov Theory

Definition [50], page 188. Consider a continuous function $V(x) : \mathbb{R}^n \to \mathbb{R}$. If there exist $R > 0$ such that $V(x_*) = 0$ and $V(x_*) > 0$ for $|x - x_*| \leq R$, $x \neq x_*$ we say that $V(x)$ is locally positive definite around x_*. If $R \to \infty$, then $V(x)$ is positive definite around x_*.

Consider the dynamical system described by an autonomous differential equation in the form,

$$\dot{x} = f(x) \tag{3.17}$$

where $x \in \mathbb{R}^n$ is the state and x_0 is the initial state. We say that $x_* \in \mathbb{R}^n$ is an equilibrium point of (3.17Stability in Sense of Lyapunov Theoryequation.3.2.17) if and only if $f(x_*) = 0$.

- x_* is stable if for each $\epsilon > 0$ there exist $\delta > 0$ such that if $|x_0 - x_*| < \delta$ then $|x(t) - x_*| < \epsilon$ for all $t \geq 0$.
- x_* is asymptotically stable if it is stable and if $|x_0 - x_*| < \delta$, then $\lim_{t\to\infty} x(t) = x_*$.

Let $V : \mathbb{X} \to \mathbb{R}$ be a continuous function such that [50],

- $V(x)$ is locally positive definite around x_*.

- If $\dot{V}(x) \leq 0$ locally in x and for all t, then the equilibrium point x_* is stable.
- If $-\dot{V}(x)$ is locally positive definite around x_* i.e. $\exists R > 0$ such that $\dot{V}(x) < 0$ for $|x - x_*| < R$ and $\dot{V}(x_*) = 0$, then the equilibrium point x_* is asymptotically stable.

Let $V : \mathbb{X} \to \mathbb{R}$ be a locally positive definite function such that on the compact set $\Omega_c = \{x \in \mathbb{X} : V(x) \leq c\}$ we have $\dot{V}(x) \leq 0$. Define the set S as,

$$S = \left\{ x \in \Omega_c : \dot{V}(x) = 0 \right\}$$

then Lasalle's principle states that if S contains no invariant sets of (3.17Stability in Sense of Lyapunov Theoryequation.3.2.17) other than $x = x_*$ then x_* is asymptotically stable [50].

3.3 Singular Perturbation Theory

Singular Perturbation Theory [11] can be used to study the behavior of a two-time scale dynamical system such as

$$\dot{x} = f(x, z, \epsilon), \quad x(t_0) = x_0 \tag{3.18}$$

$$\epsilon \dot{z} = g(x, z, \epsilon), \quad z(t_0) = z_0$$

where $x \in \mathbb{R}^n$ is the slow state variable vector, $z \in \mathbb{R}^m$ is the fast state variable vector and $0 < \epsilon \ll 1$ is the perturbation parameter that is mostly related to the ratio of fast to the slow time constants. In the limit $\epsilon \to 0$ the dynamics of the fast subsystem are assumed to converge to a steady state value characterized by the relationship $g(x, \bar{z}, 0) = 0$ resulting in $\bar{z} = \phi(x)$ and the reduced system,

$$\dot{x} = f(x, \bar{z}) = f(x, \phi(x)) \tag{3.19}$$

As a large power system contains various components and interconnections in different levels, its dynamics involves wide time span responses. There are various physical observations of time scale differences in power systems.

While performing stability analysis, including all the time scales requires complex computations and it is difficult to interpret results. However, due to wide time scale span of power systems dynamics, singular perturbation theory is applicable in many power systems stability analysis and control designs. Applying singular perturbation theory in a power system, reduced models with different approximation degrees may be developed. Chow et al. in [11] illustrates some applications of the stated time scale separation technique in power system modeling. Singular perturbation theory provides a systematic way to obtain simplified models of power systems components that have two time scales dynamics.

In a synchronous machine, inertia in the rotatory part of the sysyem results in slower dynamics compared to the electromagnetic dynamics. This physical fact and application of singular perturbation theory is the foundation of traditional automatic generation and voltage control of synchronous generators. In control of a synchronous generator it is assumed that for small changes active power depends only on internal machine angle, i.e. active power is independent of generator terminal voltage. On the other hand, the terminal voltage of synchronous generator is regulated by excitation voltage and therefore is dependent on generator's reactive power (see section 4.4Generator Controlsection.4.4). This means that for small changes, frequency and voltage can be modeled, analyzed and regulated independently. Excitation voltage control is fast acting and the transients in excitation voltage control do not have considerable influences on the slow acting power frequency control [38].

In large power systems, inter-area power transfer results in slower oscillation of groups of machines as compared to individual machines. This phenomenon is called "slow coherency" and is caused by relative strength of internal and external (in each area of machines) connections and is the basis for a coherency approach for obtaining a reduced model of power system. In this approach, first slow coherent machines that can be grouped are identified then a reduced model is constructed [11].

Various studies have developed efficient implementations of composite control strategies of singular perturbed systems such as feedback control designs that preserve the time scale structure of the system. In these approaches the fast controller is often designed first to stabilize the fast dynamics of the system and then the proper stabilizer for the slower dynamics is designed [27]. In a sequential procedure the slow controller is an inner control loop designed to stabilize the modified slower system while the frequency value of the fast controller is assumed to be zero [27, 29].

In a modern power systems such as microgrid that contains predominately inverter-based generation the natural time scale separation in traditional power systems no longer exists and it may be necessary to include all dynamics of the system in stability and performance analysis. This requires a different approach to modeling and analysis. The port-Hamiltonian formulation discussed in this dissertation is one such approach.

3.4 Control of Port-Hamiltonian Systems

Different from the traditional signal-processing approach for designing a controller, in energy perspective, the effect of a controller can be seen as a dynamical system

interconnected to the main system to modify its behavior through changes in the energy of the closed loop system.

In signal-processing controller design, the control objectives are rejecting the effect of disturbance inputs or uncertainty in inputs and plants and keeping errors in certain signals small. There is no systemic approach in designing a controller for a nonlinear system in signal-processing platform [40, 56].

In energy-based approach we concentrate on how a system behaves and interacts with its environment. Therefore, we can see a controller as another system that imposes the desired behavior on the closed loop system. The main system and its controller perceived as dynamical systems formulated in the port-Hamiltonian framework can be interconnected through power preserving interconnection laws.

Passivity-based Control (PBC), is a controller design methodology that was introduced by Ortega and Spong (1989) and achieves stabilization by shaping the energy of a passive system (3.3Passive Systemsequation.3.1.3). The control objective of PBC is to achieve a total storage function that is minimum at the desired equilibrium point [42]. For system (3.1Passive Systemsequation.3.1.1) applying the control law $u = v + \beta(x)$, the energy of the closed loop system ($H_d(x)$) is shaped to be minimum at a desired state,

$$H_d(x(t)) - H_d(x(0)) = \int_0^t v^T(\tau)y(\tau)d\tau - d_d(t) \tag{3.20}$$

where $d_d(t)$ is the dissipation of the closed loop system, i.e. if there is a function $H_a(x)$ such that,

$$-\int_0^t \beta^T(x(\tau))y(\tau)d\tau = H_a(x(t)) + \kappa \tag{3.21}$$

then with the control law $u = v + \beta(x)$ the map $v \to y$ with energy $H_d(x) = H_a(x) + H(x)$ is passive where H_a is Hamiltonian function of the controller [40].

3.4.1 Interconnection and Damping Assignment (IDA) Control

To achieve overall system stability, we shape the energy of the system to a desired function that is positive semi-definite and whose time-derivative is non-positive for any initial condition. Interconnection and damping assignment passivity based control is a method for adjusting the behavior of a nonlinear system. Using this technique we can assign a desired energy function and structure to the closed loop system [41]. The desired energy function has minimum value at the desired equilibrium point and the interconnection and damping matrices are assigned to provide the approperiate control law [41], [42]. Galaz, Ortega, et al. in [16] apply this methodology for designing the excitation control of synchronous generators.

The IDA methodology [42], considers a system of the form,

$$\dot{x} = f(x) + g(x)u \tag{3.22}$$

Assume there exist matrices $g^{\perp}(x)$, $J_d(x) = -J_d(x)^T$, $R_d(x) = R_d(x)^T$ and a function $H_d : \mathbb{R}^n \to \mathbb{R}$ that satisfies the PDE

$$g^{\perp}(x)f(x) = g^{\perp}(x)(J_d(x) - R_d(x))\nabla H_d(x) \tag{3.23}$$

where $g^{\perp}(x)$ is a full-rank left annihilator of $g(x)$, that is $g^{\perp}(x)g(x) = 0$, and $H_d(x)$ is such that

$$x_* = arg\ min\ H_d(x) \tag{3.24}$$

with $x_* \in \mathbb{R}^n$ the equilibrium to be stabilized. Then, the closed loop system with $u = \beta(x)$, where

$$\beta(x) = (g^T(x)g(x))^{-1}g^T(x)\left((J_d(x) - R_d(x))\nabla H_d(x) - f(x)\right)$$

takes the form,

$$\dot{x} = (J_d(x) - R_d(x))\nabla H_d \tag{3.25}$$

with x_* a (locally) stable equilibrium.

Solving (3.23Interconnection and Damping Assignment (IDA) Controlequation.3.4.23) in general is not an easy task. The main difference between the classical PBC and Interconnection and Damping Assignment PBC is in the design process. In classical PBC, first the desired energy function is selected then a controller that ensure this overall energy function is designed. In IDE PBC strategy, as explained, the closed loop energy function is obtained by solving (3.23Interconnection and Damping Assignment (IDA) Controlequation.3.4.23) for the desired interconnection (J_d) and damping (R_d) matrices [42].

Chapter 4

Port-Hamiltonian Systems and Power System Modeling

4.1 Port-Hamiltonian Systems' Application in Power System Modeling

An electrical power system is a composition of large number of electrical subsystems that are interconnected through appropriate topological interconnection laws.

As an object-oriented modeling, port-Hamiltonian formulation is used to model elements of power systems. Therefore, port-Hamiltonian framework provides a unified and systematic platform for expressing the dynamics of power systems' components and implementing performance and stability analysis.

Remark 4.1.1. Throughout this dissertation, we use the notation $col(a_1, a_2, .) = \begin{bmatrix} a_1 \\ a_2 \\ . \end{bmatrix}$ and $diag(a_1, a_2, .) = \begin{bmatrix} a_1 & 0 & 0 \\ 0 & a_2 & 0 \\ 0 & 0 & . \end{bmatrix}$. Furthermore, "0" and "$I$" are zero and identity matrices, respectively, whose sizes are compatible with the equation they appear in.

Example 4.1.1. Transmission Line: π model

To formulate the π model of the line in Fig. 4.1The π line modelfigure.4.1 in port-Hamiltonian framework, the states are chosen to be [15, 47], $\mathbf{x} = col(\mathbf{q_1}, \mathbf{q_2}, \boldsymbol{\phi})$, where $\mathbf{q_1}$ and $\mathbf{q_2}$ are the vectors of shunt capacitors' charges at the two ends of the line and $\boldsymbol{\phi}$ is the vector of the flux passing through the inductor. The Hamiltonian function is defined as, $\mathbf{H}_{line}(\mathbf{q_1}, \mathbf{q_2}, \boldsymbol{\phi}) = \frac{1}{2}\mathbf{x}^T M^{-1}\mathbf{x}$, where $M = diag(C_1, C_2, L)$

and C_1, C_2 and L are diagonal matrices of the line capacitance and inductance values. The gradient of Hamiltonian is, $\nabla \mathbf{H}_{line}(\mathbf{x}) = col(C_1^{-1}\mathbf{q_1}, C_2^{-1}\mathbf{q_2}, L^{-1}\boldsymbol{\phi}) = M^{-1}\mathbf{x} = col(\mathbf{v}_1, \mathbf{v}_2, \mathbf{i}_l)$.

The port-Hamiltonian model of the line is,

$$\dot{\mathbf{x}} = (\mathbf{J}_{line} - \mathbf{R}_{line})\nabla \mathbf{H}_{line} + g_{line}\mathbf{u}_{line} \tag{4.1}$$

$$\mathbf{y} = g_{line}^T \nabla \mathbf{H}_{line}(\mathbf{x}) = \begin{bmatrix} \mathbf{v_1} \\ \mathbf{v_2} \end{bmatrix}$$

where, $g_{line} = \begin{bmatrix} -I & 0 \\ 0 & I \\ 0 & 0 \end{bmatrix}$, $\mathbf{J}_{line} = \begin{bmatrix} 0 & 0 & I \\ 0 & 0 & -I \\ -I & I & 0 \end{bmatrix}$ and $\mathbf{R}_{line} = diag(G_1, G_2, R)$. The input ports' signals are the injected currents at the two nodes, i.e. $\mathbf{u}_{line} = \begin{bmatrix} \mathbf{i_1} \\ \mathbf{i_2} \end{bmatrix}$. Expressing (4.1equation.4.1.1) in form of (3.15Park-Transformationequation.3.2.15), the matrices A, B, C and D are as follows,
$A = (\mathbf{J}_{line} - \mathbf{R}_{line})M^{-1}$, $B = g_{line}$, $C = g_{line}^T M^{-1}$, $D = 0$. We define the new coordinates, $q_1 = T(\theta_r)\mathbf{q_1}$, $q_2 = T(\theta_r)\mathbf{q_2}$, $\phi = T(\theta_r)\boldsymbol{\phi}$, $v_1 = T(\theta_r)\mathbf{v_1}$, $v_2 = T(\theta_r)\mathbf{v_2}$, $\begin{bmatrix} i_1 \\ i_2 \end{bmatrix} = u_{line} = \begin{bmatrix} T(\theta_r) & 0 \\ 0 & T(\theta_r) \end{bmatrix} \mathbf{u}_{line}$, $y = \begin{bmatrix} v_1 \\ v_2 \end{bmatrix}$. Then the line dynamics in $dq0$ coordinates is,

$$\dot{x} = (\omega_r \bar{N} + A)x + Bu(t) \tag{4.2}$$

where $\bar{N} = diag(N, N, N)$, $x = col(q_1, q_2, \phi)$. For a constant input $\bar{u} = T(\theta_r)u$ the state has a steady state value $\bar{x} = (\omega_r \bar{N} + A)^{-1}B\bar{u}$ and output $\bar{y} = C\bar{x}$. In $dq0$ coordination, we define the Hamiltonian function, $H_{line}(x) = \frac{1}{2}(x - \bar{x})^T M^{-1}(x - \bar{x})$. The above function is shifted to the equilibrium point $\bar{x}$. We can rewrite the port-Hamiltonian model of the line in the new coordinates,

$$\dot{x} = (J_{line} - R_{line})\nabla H_{line}(x) + g_{line}u_{line} \tag{4.3}$$

$$y = g_{line}^T \nabla H_{line}(x) = \begin{bmatrix} v_1 - \bar{v}_1 \\ v_2 - \bar{v}_2 \end{bmatrix}$$

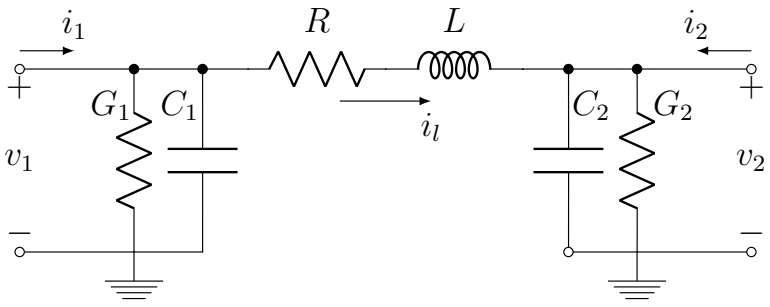

Figure 4.1: The π line model.

where $\bar{x} = col(\bar{q}_1, \bar{q}_2, \bar{\phi})$ is the equilibrium point and $\bar{q}_1 = C_1\bar{v}_1$, $\bar{q}_2 = C_2\bar{v}_2$ and $\bar{\phi} = L\bar{i}_l$,

$J_{line} = \begin{bmatrix} \omega_r NC_1 & 0 & I \\ 0 & \omega_r NC_2 & -I \\ -I & I & \omega_r NL \end{bmatrix}$ and $R_{line} = \mathbf{R}_{line}$, $u_{line} = \begin{bmatrix} i_1 - \bar{i}_1 \\ i_2 - \bar{i}_2 \end{bmatrix}$.

Remark 4.1.2. Unless otherwise stated, we assume that all the signals in the remainder of this dissertation are expressed is $dq0$ coordinates.

Example 4.1.2. Transmission Line: T model

To formulate the T model of the line in Fig. 4.2The T line modelfigure.4.2 in port-Hamiltonian framework, the states are chosen to be $\mathbf{x} = col(\boldsymbol{\phi_1}, \boldsymbol{\phi_2}, \mathbf{q})$, where $\boldsymbol{\phi_1}$ and $\boldsymbol{\phi_1}$ are the vectors of inductance's fluxes and $\mathbf{q}$ is the vector of the middle capacitor's charge. The Hamiltonian function is defined as, $\mathbf{H}_{line}(\boldsymbol{\phi_1}, \boldsymbol{\phi_2}, \mathbf{q}) = \frac{1}{2}\mathbf{x}^T M^{-1}\mathbf{x}$, where $M = diag(L_1, L_2, C)$ and L_1, L_2 and C are diagonal matrices of the line inductance and capacitance values. The gradient of Hamiltonian is, $\nabla\mathbf{H}_{line}(\mathbf{x}) = col(L_1^{-1}\boldsymbol{\phi_1}, L_2^{-1}\boldsymbol{\phi_1}, C^{-1}\mathbf{q}) = M^{-1}\mathbf{x} = col(\mathbf{i}_1, \mathbf{i}_2, \mathbf{v}_l)$.

The port-Hamiltonian model of the line is,

$$\dot{\mathbf{x}} = (\mathbf{J}_{line} - \mathbf{R}_{line})\nabla\mathbf{H}_{line} + g_{line}\mathbf{u}_{line} \tag{4.4}$$

$$\mathbf{y} = g_{line}^T \nabla\mathbf{H}_{line}(\mathbf{x}) = \begin{bmatrix} \mathbf{i_1} \\ \mathbf{i_2} \end{bmatrix}$$

where, $g_{line} = \begin{bmatrix} -I & 0 \\ 0 & I \\ 0 & 0 \end{bmatrix}$, $\mathbf{J}_{line} = \begin{bmatrix} 0 & 0 & I \\ 0 & 0 & -I \\ -I & I & 0 \end{bmatrix}$ and $\mathbf{R}_{line} = diag(R_1, R_2, G)$. The input ports' signals are the enforced voltages at the two nodes, $\mathbf{u}_{line} = \begin{bmatrix} \mathbf{v_1} \\ \mathbf{v_2} \end{bmatrix}$. Expressing (4.4equation.4.1.4) in form of (3.15Park-Transformationequation.3.2.15), the matrices A, B, C and D are as follows,

$A = (\mathbf{J}_{line} - \mathbf{R}_{line})M^{-1}$, $B = g_{line}$, $C = g_{line}^T M^{-1}$, $D = 0$. We define the new coordinates, $\phi_1 = T(\theta_r)\boldsymbol{\phi_1}$, $\phi_2 = T(\theta_r)\boldsymbol{\phi_2}$, $q = T(\theta_r)\mathbf{q}$, $i_1 = T(\theta_r)\mathbf{i_1}$, $i_2 = T(\theta_r)\mathbf{i_2}$, $\begin{bmatrix} v_1 \\ v_2 \end{bmatrix} = u_{line} = \begin{bmatrix} T(\theta_r) & 0 \\ 0 & T(\theta_r) \end{bmatrix} \mathbf{u}_{line}$, $y = \begin{bmatrix} i_1 \\ i_2 \end{bmatrix}$. Then the line dynamics in $dq0$ coordinates is,

$$\dot{x} = (\omega_r \bar{N} + A)x + Bu(t) \tag{4.5}$$

where $\bar{N} = diag(N, N, N)$, $x = col(\phi_1, \phi_2, q)$. For a constant input $\bar{u} = T(\theta_r)u$ the state has a steady state value $\bar{x} = (\omega_r \bar{N} + A)^{-1} B\bar{u}$ and output $\bar{y} = C\bar{x}$. In $dq0$ coordination, we define the Hamiltonian function, $H_{line}(x) = \frac{1}{2}(x - \bar{x})^T M^{-1}(x - \bar{x})$. The above function is shifted to the equilibrium point $\bar{x}$. We can rewrite the port-Hamiltonian model of the line in the new coordinates,

$$\dot{x} = (J_{line} - R_{line})\nabla H_{line}(x) + g_{line} u_{line} \tag{4.6}$$

$$y = g_{line}^T \nabla H_{line}(x) = \begin{bmatrix} i_1 - \bar{i}_1 \\ i_2 - \bar{i}_2 \end{bmatrix}$$

where $\bar{x} = col(\bar{\phi}_1, \bar{\phi}_2, \bar{q})$ is the equilibrium point and $\bar{\phi}_1 = L_1\bar{i}_1$, $\bar{\phi}_2 = L_2\bar{i}_2$ and $\bar{q} = C\bar{v}_l$,
$J_{line} = \begin{bmatrix} \omega_r N L_1 & 0 & I \\ 0 & \omega_r N L_2 & -I \\ -I & I & \omega_r N C \end{bmatrix}$ and $R_{line} = \mathbf{R}_{line}$, $u_{line} = \begin{bmatrix} v_1 - \bar{v}_1 \\ v_2 - \bar{v}_2 \end{bmatrix}$.

Remark 4.1.3. In the π model of a line the input port variable is current and the output is voltage. Consequently, the π line model would be connected to a source whose output is current, i.e. a "current source". On the other hand, the

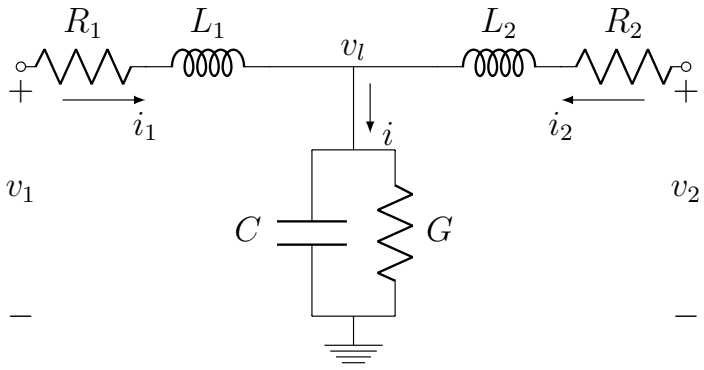

Figure 4.2: The T line model.

input port variable for the T model of a line is voltage and thus the T line model would be connected to a source that is a "voltage source".

Example 4.1.3. Network

The port-Hamiltonian model of an electrical network of interconnected π lines as in Fig 4.1The π line modelfigure.4.1 in presented in [47]. The lines' interconnection matrix is $D \in \mathbb{R}^{n_C \times n_L}$ where n_C is the number of capacitors and n_L is the number of inductors in the network. The capacitors' charges $Q(t) \in \mathbb{R}_{n_C}$ and the inductors' fluxes $\phi(t) \in \mathbb{R}_{n_L}$ are the states $x(t) = \begin{bmatrix} Q(t) \\ \phi(t) \end{bmatrix}$ and the Hamiltonian function of the network is a quadratic function of states:

$$H(x(t)) = \frac{1}{2} x^T(t) \begin{bmatrix} C^{-1} & 0 \\ 0 & L^{-1} \end{bmatrix} x(t)$$

where C, L and R are the diagonal matrices of capacitance, inductance and resistance values of the network, respectively. The port-Hamiltonian model of the network is:

$$\begin{bmatrix} \dot{Q}(t) \\ \dot{\phi}(t) \end{bmatrix} = (J - R)\nabla H(Q(t), \phi(t)) + \begin{bmatrix} I_{n_C \times n_C} & 0 \\ 0 & 0 \end{bmatrix} i(t)$$

$$y(t) = \begin{bmatrix} I_{n_C \times n_C} & 0 \\ 0 & 0 \end{bmatrix}^T \nabla H(x(t)) = v(t) \tag{4.7}$$

where $\nabla H(x(t)) = \begin{bmatrix} C^{-1}Q(t) \\ L^{-1}\phi(t) \end{bmatrix} = \begin{bmatrix} v(t)_{n_C \times 1} \\ i_l(t)_{n_L \times 1} \end{bmatrix}$ and $J = \begin{bmatrix} 0 & D \\ -D^T & 0 \end{bmatrix}$. The signals in the above formulation are three phase sinusoidal signals. Applying the Park transformation (section 3.2.1Park-Transformationsubsection.3.2.1) to the dynamic equation (4.7equation.4.1.7) the transformed states are,

$$\bar{x} = \breve{T}(\theta_r) \begin{bmatrix} Q_t \\ \phi(t) \end{bmatrix} = \begin{bmatrix} \bar{Q}_t \\ \bar{\phi}(t) \end{bmatrix}$$

where $\breve{T}(\theta_r) = (\underbrace{T(\theta_r), ..., T(\theta_r)}_{n_c \times n_L})$. The interconnection matrix,

$$\breve{J} = \omega_r \breve{N} \begin{bmatrix} C & 0 \\ 0 & L \end{bmatrix} + J$$

where $\breve{N} = (\underbrace{N, ..., N}_{n_c \times n_L})$. the damping matrix is unchanged, i.e. $\breve{R} = R$.

Example 4.1.4. Synchronous Generator Port-Hamiltonian Modeled as Current Source

In this section we briefly review the dynamic equations of synchronous generator and demonstrate that it can be viewed as a dynamic voltage controlled current source.

The swing equation of a synchronous generator describes the rotational dynamics of the machine

$$J\dot{\omega} = T_m - T_e \tag{4.8}$$

and we also have,

$$\dot{\theta}_d = \omega \tag{4.9}$$

In the equation above, T_m is the input mechanical torque and T_e is the electrical torque. When the frequency is regulated to its nominal value $\omega = \omega_r$, $T_e = T_m$.

The electrical equations of synchronous generators for the a coordinate (b and c coordinates are similar) are

$$\lambda_a = L_s i_a - M_s i_b - M_s i_c + M_f cos(\theta_d) i_f = (L_s + M_s) i_a + M_f cos(\theta_d) i_f$$

and the terminal voltage for phase a,

$$v_a = -R_s i_a - \frac{d\lambda_a}{dt}$$

Here, λ_a is the flux linkage of phase a and θ_d is the angle between generator a axis and d axis of its rotor. The angle between the d axis and b and c generator axes are $\theta_d - \frac{2\pi}{3}$ and $\theta_d - \frac{4\pi}{3}$, respectively. The field (rotor) circuit satisfies

$$\lambda_f = L_{ff} i_f + M_f cos(\theta_d) i_a + M_f cos(\theta_d - \frac{2\pi}{3}) i_b + M_f cos(\theta_d - \frac{4\pi}{3}) i_c$$

and

$$v_f = R_f i_f + \frac{d\lambda_f}{dt}$$

We collect the above equations into a vector differential equation, i.e. $\begin{bmatrix} \lambda_{abc} \\ \lambda_f \end{bmatrix} = \begin{bmatrix} \lambda_a & \lambda_b & \lambda_c & \lambda_f \end{bmatrix}^T$, etc. and transform the resulting system into a rotating coordinate system defined by the system frequency ω_r. Note that the field variables are not transformed. The system equations in a port-Hamiltonian formulation have the form (see, e.g. [47])

$$\dot{\bar{\lambda}} = (J(\omega_r) - R)\nabla H(\bar{\lambda}) - M(\omega_r)\bar{i} - \bar{v} \tag{4.10}$$

$$= (N(\omega_r) - R)\nabla H(\bar{\lambda}) - \bar{v}$$

where the Hamiltonian function is defined as

$$H(\bar{\lambda}) = \frac{1}{2}\bar{\lambda}^T \bar{L}^{-1} \bar{\lambda} \tag{4.11}$$

and $\bar{v} = \begin{bmatrix} \bar{v}_t \\ -v_f \end{bmatrix}$, $\bar{v}_t$ is the generator terminal voltage and v_f the field voltage. The system matrices in (4.10equation.4.1.10) and (4.11equation.4.1.11) are

$$N(\omega_r) = \omega_r \begin{bmatrix} 0 & -(L_s + M_s) & -\sqrt{\frac{3}{2}} M_f sin(\Delta\theta) \\ L_s + M_s & 0 & \sqrt{\frac{3}{2}} M_f cos(\Delta\theta) \\ 0 & 0 & 0 \end{bmatrix},$$

$$\bar{J}(\omega_r) = \omega_r \begin{bmatrix} 0 & -(L_s + M_s) & 0 \\ L_s + M_s & 0 & 0 \\ 0 & 0 & 0 \end{bmatrix},$$

$$M(\omega_r) = \omega_r \begin{bmatrix} 0 & 0 & -\sqrt{\frac{3}{2}} M_f sin(\Delta\theta) \\ 0 & 0 & \sqrt{\frac{3}{2}} M_f cos(\Delta\theta) \\ 0 & 0 & 0 \end{bmatrix},$$

$\bar{L} = \begin{bmatrix} (L_s + M_s)I & L_{fm} \\ L_{fm}^T & L_{ff} \end{bmatrix}$, $R = \begin{bmatrix} R_s I & 0 \\ 0 & R_f \end{bmatrix}$, $L_{fm} = \sqrt{\frac{3}{2}} M_f \begin{bmatrix} cos(\Delta\theta) & sin(\Delta\theta) \end{bmatrix}^T$ where $\bar{\lambda}_t$ is the vector of armature flux, L_s and M_s the armature self inductance and mutual inductance, L_{ff} is the field coil self inductance and M_f is related to the armature and field mutual inductance, $\Delta\theta = \theta_r - \theta_d$, $\theta_d = \omega t + \theta_{d0}$, $\theta_r = \omega_r t$, θ_{d0} is the "initial" generator angle. In the above model, the output is

$$y = -\nabla H(\bar{\lambda}) = -\begin{bmatrix} \bar{i}_t \\ i_f \end{bmatrix} \tag{4.12}$$

We note that due to that fact that 0 element in the transformed of three phase balanced signals in $dq0$ coordinates has null value, in the above formulation we have dropped the "0" coordinate in $dq0$. Evaluating (4.10equation.4.1.10)-(4.12equation.4.1.12) in steady state gives the steady state model of the synchronous generator,

$$i_s = (N(\omega_r) - R)^{-1} v_s \tag{4.13}$$

i.e. in steady state the generator has the form of a voltage controlled current source.

One control goal of typical generator controllers in power systems is to regulate the generator terminal voltage. We can rewrite the steady state relationship as

$$v_s = (N(\omega_r) - R)i_s \tag{4.14}$$

We note that this relationship does not directly correspond to the synchronous generator dynamical system, i.e. the role of the dependent (output) and independent (input) variables has been interchanged in the steady state relationship.

Remark 4.1.4. Conventional voltage source models of synchronous generator (voltage source behind reactance) are based on the inverse relationship (4.14equation.4.1.14).

Example 4.1.5. Synchronous Generator Port-Hamiltonian Modeled as Voltage Source

We are interested in developing a dynamic voltage source, i.e. a causal system that mimics the synchronous generator that has current as input and voltage as output. One such system is a so-called electrostatic generator which is essentially the dual of a synchronous machine [17, 34]. In particular, consider the machine in Fig. 4.3Electrical Circuit of Three-phase Electrostatic Generatorfigure.4.3 which has mathematical description for the a-phase

$$q_a = C_s v_a - C_m v_b - C_m v_c + N_f cos(\theta_d) v_f = (C_s + C_m) v_a + N_f cos(\theta_d) v_f$$

where q_a is the charge of phase a and

$$i_a = -G_s v_a - \dot{q}_a$$

where the b and c phases are described by similar equations with phase differences $-\frac{2\pi}{3}$ and $-\frac{4\pi}{3}$. The "field" equation has the form

$$q_f = C_f v_f + C_{rs}^T v_{abc}$$

where $C_{rs} = N_f \begin{bmatrix} cos(\theta_d) & cos(\theta_d - \frac{2\pi}{3}) & cos(\theta_d - \frac{4\pi}{3}) \end{bmatrix}^T$. In three phase vector format we have

$$q_{abc} = (C_s + C_m)v_{abc} + C_{rs}v_f$$

$$i_{abc} = -G_s v_{abc} - \dot{q}_{abc}$$

$$i_f = G_f v_f + \dot{q}_f$$

We note that in this model C_s is self capacitance while C_m and C_{rs} are mutual capacitances. After transferring all the signals to rotational coordinates at the system frequency ω_r

$$\dot{q}_{dq} = -G_s \bar{v}_t + N q_{dq} - \bar{i}_t$$

$$\dot{q}_f = -G_f v_f + i_f$$

where ${C'_{rs}}^T = \sqrt{\frac{3}{2}} N_f \begin{bmatrix} cos(\Delta\theta) & sin(\Delta\theta) \end{bmatrix}$, $\bar{q} = \begin{bmatrix} q_{dq}^T & q_f \end{bmatrix}^T$. Define the Hamiltonian function as the total energy stored in the capacitors, i.e. $H' = \frac{1}{2}\bar{q}^T C^{-1} \bar{q}$, then the dynamics of electrostatic generator

$$\dot{\bar{q}} = (J'(\omega_r) - R')\nabla H'(q) + g\bar{i} \tag{4.15}$$

$$\bar{v} = g^T \nabla H'$$

where $\bar{i} = \begin{bmatrix} \bar{i}_t^T & i_f \end{bmatrix}^T$, $g = \begin{bmatrix} -I & 0 \\ 0 & 1 \end{bmatrix}$, $\bar{v} = \begin{bmatrix} -\bar{v}_t^T & v_f \end{bmatrix}^T$, $\nabla H' = C^{-1}\bar{q}$.

$$C = \begin{bmatrix} (C_s + C_m)I & C'_{rs} \\ {C'_{re}}^T & C_f \end{bmatrix}$$

$$J'(\omega_r) - R' = \begin{bmatrix} -G_s & -(C_s + C_m)\omega_r & -\sqrt{\frac{3}{2}} N_f \omega_r sin(\Delta\theta) \\ (C_s + C_m)\omega_r & -G_s & \sqrt{\frac{3}{2}} N_f \omega_r cos(\Delta\theta) \\ 0 & 0 & -G_f \end{bmatrix}$$

As in the synchronous generator model we have dropped the "0" component of $dq0$ signals. The rotational dynamics for the electrostatic generator are identical to

those of the traditional synchronous machine. In steady state the system equation (4.15equation.4.1.15) takes the form,

$$v_s = -g^{-1}(J'(\omega_r) - R')^{-1} i_s \tag{4.16}$$

i.e. it is a current controlled voltage source. It is of interest to investigate under what conditions steady state output (4.16equation.4.1.16) corresponds to the non-causal steady state relationship (4.14equation.4.1.14). In practice if we equate equations (4.16equation.4.1.16) and (4.14equation.4.1.14), resulting in

$$G_f = \frac{1}{R_s}, G_s = \frac{R_s}{K}, C_s = -\frac{L_s}{K}, C_m = -\frac{M_s}{K}, N_f = -\frac{M_f}{R_f\sqrt{K}}$$

where $K = (L_s + M_s)^2\omega_r^2 + R_s^2$. We note, in particular that the inductance values are negative which corresponds to the fact that (4.14equation.4.1.14) corresponds to an anti-causal machine.

For various technical reasons the electrostatic generator described earlier cannot be built as an efficient power generator. There are however, several applications of such machines as MEMS devices [22, 28].

4.2 Load Models

As loads play an important role in the analysis of voltage instabilities in power systems, aggregating proper load models in stability analyses is crucial [20]. As static load models are not sufficient for these analyses, dynamic models are required. In this section we review the port-Hamiltonian model of constant impedance loads [47] and express the dynamics of induction motors in port-Hamiltonian formulation. Furthermore, we propose a port-Hamiltonian model for Constant Power Loads (CPLs). As a starting point we note that any port-Hamiltonian load model has

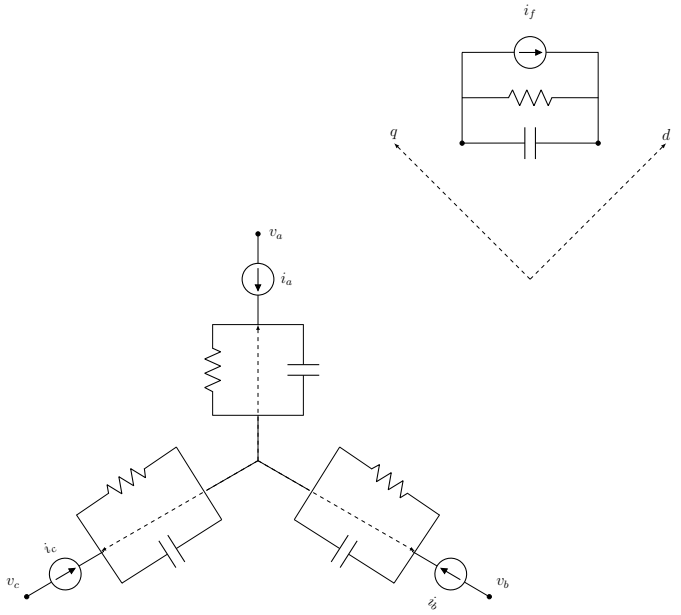

Figure 4.3: Electrical Circuit of Three-phase Electrostatic Generator.

the standard form,

$$\dot{x} = (J(x) - R(x))\nabla H(x) + Bv_l + Eu \tag{4.17}$$

$$i_l = B^T \nabla H(x)$$

where v_l and i_l are the load terminal voltage and current. $H(x)$ is a Hamiltonian function, $J_x = -J^T(x)$ and $R_x = R^T(x) \geq 0$ are appropriately chosen interconnection and damping matrices, and u is an external input variable that can be a complex function of the system state, terminal variables and other external variables.

4.2.1 Constant Impedance Load

Considering the port-Hamiltonian model of the inductive load shown in Fig. 4.4The inductive load modelfigure.4.4, we select ϕ_l, the vector of the inductive load flux

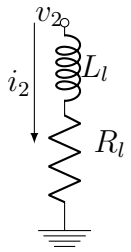

Figure 4.4: The inductive load model.

as state variable for the Hamiltonian function as [47],

$$H_{load} = \frac{1}{2}(\phi_l - L_l\bar{i}_2)^T L_l^{-1}(\phi_l - L_l\bar{i}_2) \tag{4.18}$$

where L_l is the load inductance and $\bar{i}_2$ is the load current at an equilibrium point. The load flux at the equilibrium is, $\bar{\phi}_l = L_l\bar{i}_2$. The port-Hamiltonian model is,

$$\dot{x} = (J_{load} - R_{load})\ \nabla H_{load} + g_{load}u_{load} \tag{4.19}$$

$$y = g_{load}^T u_{load} = i_2 - \bar{i}_2$$

where J_{load} and R_{load} are the load interconnection and dissipation matrices, respectively. Here, $J_{load} = \omega_r N L_l$ and $R_{load} = R_l$ and it is easy to see that $J_{load}^T = -J_{load}$ and $R_{load}^T = R_{load}$. Finally, $g_{load} = I$ and $u_{load} = v_2 - \bar{v}_2$, where v_2 and $\bar{v}_2$ are the vector of load voltage and its steady state value.

4.2.2 Induction Motor Load

The electrical equations of phase a of stator and rotor of a doubly fed induction generator in sinusoidal three phase are,

$$\lambda_{sa} = (l_{ls} + l_{ms})i_{sa} + (-\frac{1}{2}l_{ms})i_{sb} + (-\frac{1}{2}l_{ms})i_{sc} \tag{4.20}$$

$$+M[cos(\theta_r)i_{ra} + cos(\theta_r - \frac{2\pi}{3})i_{rb} + cos(\theta_r - \frac{4\pi}{3})i_{rc}]$$

$$\lambda_{ra} = (l_{lr} + l_{ms})i_{ra} + (-\frac{1}{2}l_{ms})i_{rb} + (-\frac{1}{2}l_{ms})i_{rc} \tag{4.21}$$
$$+M[cos(\theta_r)i_{sa} + cos(\theta_r - \frac{2\pi}{3})i_{sb} + cos(\theta_r - \frac{4\pi}{3})i_{sc}]$$

The same equations can be written for the other coils of the stator and rotor. In all the formulas, rotor variables are returned to the stator side. The voltage drop for the coil a of stator and rotor

$$v_{sa} = R_s i_{sa} + \frac{d\lambda_{sa}}{dt} \tag{4.22}$$

$$v_{ra} = R_r i_{ra} + \frac{d\lambda_{ra}}{dt} \tag{4.23}$$

Combining all above equations gives

$$\lambda = L(\theta_r)i$$

$$\dot{\lambda} = -Ri + v$$

where $L(\theta_r) = \begin{bmatrix} L_s & L_{sr} \\ L_{sr}^T & L_r \end{bmatrix}$

$$L_s = \begin{bmatrix} l_{ls} + l_{ms} & -\frac{l_{ms}}{2} & -\frac{l_{ms}}{2} \\ -\frac{l_{ms}}{2} & l_{ls} + l_{ms} & -\frac{l_{ms}}{2} \\ -\frac{l_{ms}}{2} & -\frac{l_{ms}}{2} & l_{ls} + l_{ms} \end{bmatrix}$$

$$L_r = \begin{bmatrix} l_{lr} + l_{ms} & -\frac{l_{ms}}{2} & -\frac{l_{ms}}{2} \\ -\frac{l_{ms}}{2} & l_{lr} + l_{ms} & -\frac{l_{ms}}{2} \\ -\frac{l_{ms}}{2} & -\frac{l_{ms}}{2} & l_{lr} + l_{ms} \end{bmatrix}$$

$L_{sr} = M \begin{bmatrix} cos(\theta_r) & cos(\theta_r - \frac{2\pi}{3}) & cos(\theta_r - \frac{4\pi}{3}) \\ cos(\theta_r - \frac{4\pi}{3}) & cos(\theta_r) & cos(\theta_r - \frac{2\pi}{3}) \\ cos(\theta_r - \frac{2\pi}{3}) & cos(\theta_r - \frac{4\pi}{3}) & cos(\theta_r) \end{bmatrix}$, $\theta_r(t) = \Omega_r(t) + \theta_{r_0}$

$R = \begin{bmatrix} R_s I & 0 \\ 0 & R_r I \end{bmatrix}$, $\lambda = \begin{bmatrix} \lambda_s \\ \lambda_r \end{bmatrix}$, $v = \begin{bmatrix} v_s \\ v_r \end{bmatrix}$ and $i = \begin{bmatrix} i_s \\ i_r \end{bmatrix}$ where the subscript s and r are denoted to stator and rotor, respectively. The transformation matrix for transforming the above equations to stationary frame is,

$$\Upsilon = \begin{bmatrix} T(\Omega_s t) & 0 \\ 0 & T(\Omega_r t) \end{bmatrix} \tag{4.24}$$

where $\Omega_s = \Omega_r + \Delta\Omega$, Ω_r is rotor frequency and Ω_s is stator frequency. $\Delta\Omega$ is a fixed design value chosen as desired slip. The equations in $dq0$ coordinates are,

$$\begin{bmatrix} \dot{\bar{\lambda}}_s \\ \dot{\bar{\lambda}}_r \end{bmatrix} = \begin{bmatrix} \Omega_s N & 0 \\ 0 & \Omega_r N \end{bmatrix} \bar{L}\bar{i} - R\bar{i} + \bar{v} \tag{4.25}$$

$$\bar{L} = T\Upsilon L(\theta_r)\Upsilon^T = \begin{bmatrix} \bar{L}_s & \bar{L}_{sr} \\ \bar{L}_{sr}^T & \bar{L}_r \end{bmatrix}, \quad \bar{L}_s = (l_{ls} + \frac{3l_{ms}}{2})I$$

$$\bar{L}_r = (l_{lr} + \frac{3l_{ms}}{2})I, \quad \bar{L}_{sr} = \frac{3l_{ms}}{2}I$$

$$\begin{bmatrix} \Omega_s N & 0 \\ 0 & \Omega_r N \end{bmatrix} \bar{L} = \begin{bmatrix} \Omega_s N\bar{L}_s & \Omega_s N\bar{L}_{sr} \\ \Omega_r N\bar{L}_{sr}^T & \Omega_r N\bar{L}_r \end{bmatrix}$$

$$= \begin{bmatrix} \Omega_s N\bar{L}_s & \Omega_s N\bar{L}_{sr} \\ (\Omega_s + \Delta\Omega)N\bar{L}_{sr}^T & (\Omega_s + \Delta\Omega)N\bar{L}_r \end{bmatrix}$$

$$= \Omega_s N\bar{L} + \begin{bmatrix} 0 & 0 \\ \Delta\Omega N\bar{L}_{sr}^T & \Delta\Omega N\bar{L}_r \end{bmatrix}$$

$$= \Omega_s N\bar{L} + M(\Delta\Omega)$$

and $\Omega_s = \omega_r$.

The port-Hamiltonian model of a doubly fed induction generator has the form,

$$\begin{bmatrix} \dot{\bar{\lambda}}_s \\ \dot{\bar{\lambda}}_r \end{bmatrix} = (\omega_r N\bar{L} - R)\bar{i} - M(\Delta\Omega)\bar{i} + \bar{v} \tag{4.26}$$

$$\bar{y} = \bar{i} \tag{4.27}$$

The Hamiltonian function for the model is $H = \frac{1}{2}\bar{\lambda}^T\bar{L}^{-1}\bar{\lambda}$ and its gradient is $\nabla H = \bar{L}^{-1}\bar{\lambda} = \bar{i}$. We note that if we include the $\Delta\Omega$ dynamics the motor model has the general port-Hamiltonian form of a load.

4.2.3 Constant Power Load

CPLs that consist of solid-state self-regulated power electronic devices are increasing in power systems. The strong nonlinear behavior that CPLs introduces new

challenges in dynamical studies of power systems. Due to the fast dynamics of CPLs the application of standard singular perturbation theory (section 3.3Singular Perturbation Theorysection.3.3) for neglecting load dynamics is not valid.

Allen and Ilic in [2] show that applying a static or slow dynamic model for PQ loads while including the transmission line dynamics results in instabilities around the desired load flow solution. A simple dynamic representation of CPLs can be found in [1, 2, 43],

$$\dot{g} = \frac{1}{\tau}\left[P_{ref} - \frac{|i_l|^2}{g}\right] \tag{4.28}$$

where P_{ref} is the constant real power that load is expected to consume, g is the conductance value of the load and its conductance matrix is as $G = gI$ and i_l is the load port current in $dq0$ coordinates. The PQ load model in [2] includes a dynamic susceptance part (B) for an admittance in the form $G + jB$ as well.

The CPL dynamics in (4.28Constant Power Loadequation.4.2.28) for a relatively long time constant behaves as a constant impedance load. As is shown in [2] there is a critical value of τ for which the system obtain from the load (4.28Constant Power Loadequation.4.2.28) connected to a transmission line becomes unstable. Consequently for short time constants, the CPL model in (4.28Constant Power Loadequation.4.2.28) results in instabilities and therefore, this model is not a good representation of CPL dynamics where time constants are typically very small.

At the load input terminal, CPLs acts like a negative incremental impedance. For constant power of the load, the current and voltage at terminals,

$$|i_l| = \frac{P_{ref}}{|v_l|} \tag{4.29}$$

by (4.29Constant Power Loadequation.4.2.29)the voltage drop causes increase in the current. Therefore, to study small signal stability, some papers apply a negative impedance model for CPLs. This equiavalent impedance of CPLs may be used in impedance-based small signal stability analysis [44, 45, 53].

Proposed Constant Power Load

A model for Constant Power load is proposed in the standard port-Hamiltonian formulation,

$$\dot{x} = (J_l(x) - R_l(x))\nabla H(x) + v_l + Eu \tag{4.30}$$

$$y = i_l = \Pi x$$

where the Hamiltonian function is,

$$H(x) = \frac{1}{2}x^T \Pi x \tag{4.31}$$

where $R_l(x)$ is symmetric positive semi-definite, $J_l(x)$ is skew symmetric, $\Pi = \Pi^T > 0$. The control variable u is the output of a controller that regulates the active power, e.g.

$$u = C(s)(P_{ref} - P) \tag{4.32}$$

the power P in the above formulation is $P = i_l^T v_l$ where i and v are the output and input ports of the CPL port-Hamiltonian model. Fig 4.6Block diagram of the proposed CPL modelfigure.4.6 shows the designed block diagram of CPL. The control law $C(s)$ in (4.32Proposed Constant Power Loadequation.4.2.32) is chosen so that $P(t) \to P_{ref}$ when v_l is at any steady state value. The matrices in (4.30Proposed Constant Power Loadequation.4.2.30) are chosen by identification of the dynamics of the load being modeled. For illustrative purposes we performed a simulation for the above constant power load model. The matrices in our model are constant and

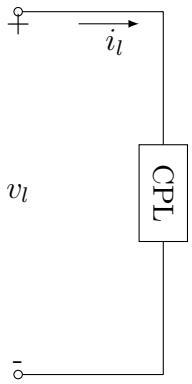

Figure 4.5: Constant power load.

the controller for the chosen load is selected as a PID controller. Fig. 4.7The active power of CPL when there is a 20% drop in its terminal voltagefigure.4.7 shows the output power of CPL when there is a voltage drop of 20% at the load terminal as seen in Fig. 4.8A 20% drop in terminal voltage of the modeled CPLfigure.4.8.

The reactive power at the load terminal is,

$$Q = i^T N v \tag{4.33}$$

where N is as before $\begin{bmatrix} 0 & -1 & 0 \\ 1 & 0 & 0 \\ 0 & 0 & 0 \end{bmatrix}$. In the proposed load model (4.30Proposed Constant Power Loadequation.4.2.30) at steady state we have,

$$\begin{aligned} 0 &= i_{l_s}^T N(J_l(x_s) - R_l(x_s))\nabla H(x_s) + i_{l_s}^T N v_{l_s} + i_{l_s}^T N E u_s \\ &= i_{l_s}^T N J_l(x_s) i_{l_s} + Q + i_{l_s}^T N E u_s = 0 \end{aligned} \tag{4.34}$$

For simplicity assume $J_l = \alpha N$ for some constant α (note that in dq coordinates J_l always has the form $J_l = \omega_r N + J_1$ where J_1 is skew symmetric). In this case,

$$Q = -\alpha |i_{l_s}|^2 - i_{l_s}^T N E u_s \tag{4.35}$$

and the second term in (4.34Proposed Constant Power Loadequation.4.2.34) is,

$$i_{l_s}^T N E u_s = i_{l_s}^T N E C(0)(P_{ref} - P_s)$$

For good regulation of active power this term is relatively small.

The active power can be written as,

$$P = |i||v|cos(\theta) \tag{4.36}$$

where for a load, $cos(\theta)$ is the power factor. If $P_{ref} > 0$ we must have $cos(\theta) > 0$ and thus $\theta \in \left[-\frac{\pi}{2}, \frac{\pi}{2}\right]$. Consequently,

$$\frac{\partial |i_l|}{\partial |v_l|} = -\frac{P_{ref}}{|v_l|^2 cos(\theta)} < 0 \tag{4.37}$$

which agrees with the statement that the negative impedance claim in [44, 45, 53]. If we look at the reactive power for $\theta \in \left[-\frac{\pi}{2}, \frac{\pi}{2}\right]$ we see that for $\theta \in \left[-\frac{\pi}{2}, 0\right]$, $Q = |i||v|sin(\theta) < 0$ i.e. the system looks like a capacitive load while for $\theta \in \left[0, \frac{\pi}{2}\right]$, $Q > 0$ and the load looks inductive.

Note that in (4.30Proposed Constant Power Loadequation.4.2.30) for $\alpha > 0$ we have from (4.35Proposed Constant Power Loadequation.4.2.35) that $Q > 0$ while for $\alpha < 0$ we have $Q < 0$. Thus (4.30Proposed Constant Power Loadequation.4.2.30) can be selected to produce capacitive or inductive type of load by choice of the interconnection matrix J_l. Fig 4.9The reactive power of the modeled CPL for different values of αfigure.4.9 illustrates the reactive power of the modeled CPL for different values of α that model inductive ($Q > 0$) or capacitive ($Q < 0$) or resistive ($Q = 0$) loads.

4.3 Passivity of inductive loads and network

The Hamiltonian function for a system that includes inductive loads and network (example 4.1.3exmp.4.1.3 and section 4.2.1Constant Impedance Loadsubsection.4.2.1), has the quadratic form

$$H_n(x_n) = \frac{1}{2} x_n^T M x_n \tag{4.38}$$

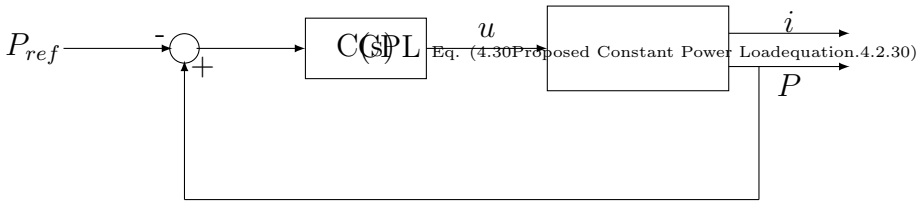

Figure 4.6: Block diagram of the proposed CPL model.

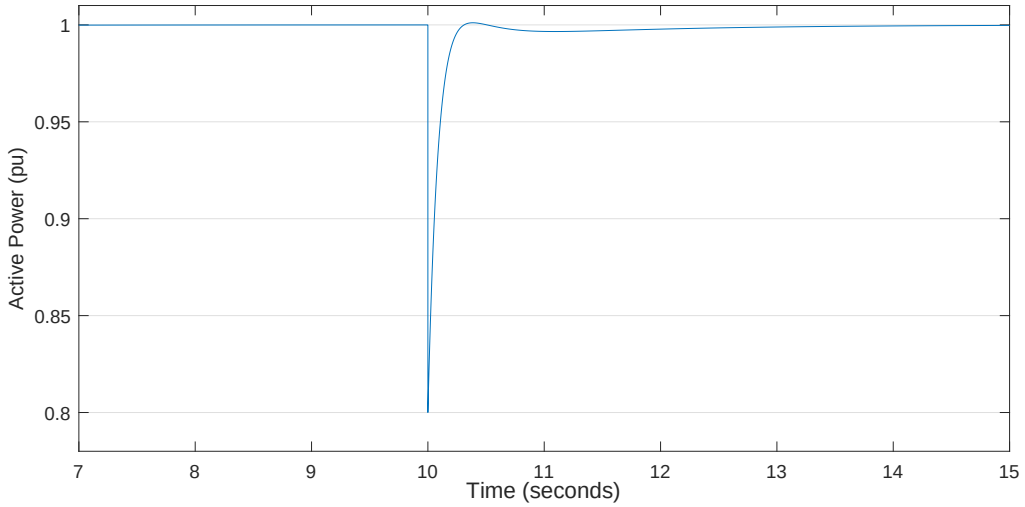

Figure 4.7: The active power of CPL when there is a 20% drop in its terminal voltage.

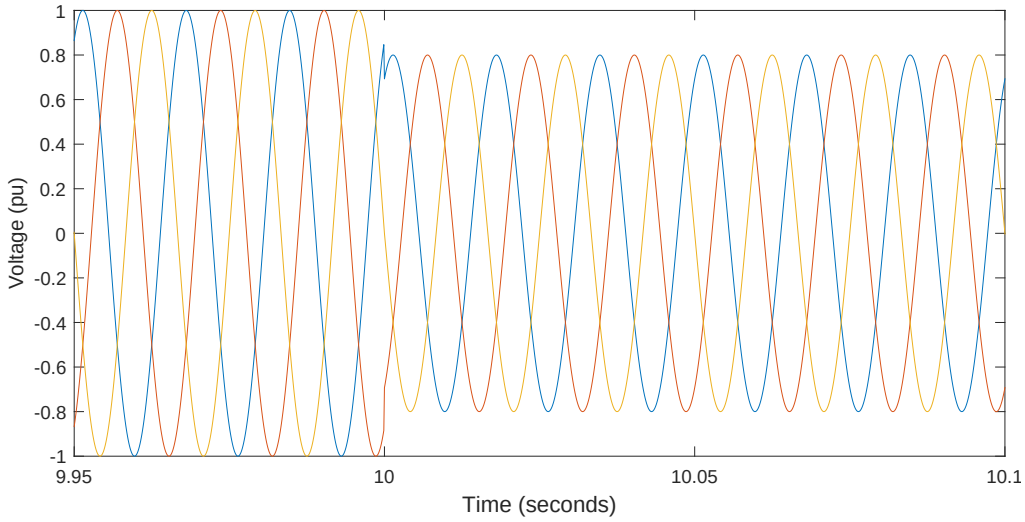

Figure 4.8: A 20% drop in terminal voltage of the modeled CPL.

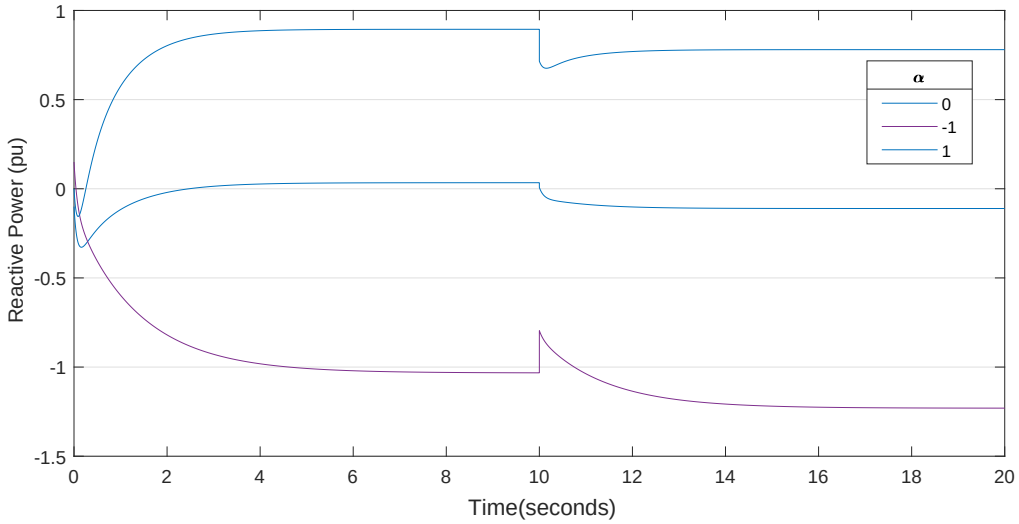

Figure 4.9: The reactive power of the modeled CPL for different values of α.

where x_n includes the fluxes of lines and inductive loads and charges of capacitors and

$$M = \begin{bmatrix} C^{-1} & 0 & 0 \\ 0 & L_l^{-1} & 0 \\ 0 & 0 & L_d^{-1} \end{bmatrix}$$

We can rewrite this system in the form

$$\dot{x}_n = (J_n(x_n) - R_n(x_n))Mx_n + g_n(x_n)u_n + e_n(x_n)v_n \tag{4.39}$$

$$y_n = g_n^T(x_n)Mx_n$$

Evaluating inequality (3.6equation.3.1.6) in proposition 3.1.1prop.3.1.1 for (4.39Passivity of inductive loads and networkequation.4.3.39) gives,

$$\nabla H_n^T(x_n)(J_n(x_n) - R_n(x_n))Mx_n = -x_n^T M R_n(x_n) M x_n \leq 0$$

and (3.7equation.3.1.7) also holds for port-Hamiltonian system (4.39Passivity of inductive loads and networkequation.4.3.39). Therefore, system (4.39Passivity of inductive loads and networkequation.4.3.39) is passive.

4.3.1 Incremental system of inductive load and network

Let x_n^* be an equilibrium state of the system (4.39Passivity of inductive loads and networkequation.4.3.39) and define the incremental variables,

$$\tilde{x}_n = x_n - x_n^*$$

$$\tilde{u}_n = u_n - u_n^*$$

$$\tilde{y}_n = y_n - y_n^*$$

We know that at the equilibrium state x_n^*, we have,

$$(J_n - R_n)\nabla H_n(x_n^*) + g_n u_n^* = 0 \tag{4.40}$$

Remark 4.3.1. For the system consisting of inductive loads and network the interconnection and damping matrices are constant.

Since H_n is in the form (4.38Passivity of inductive loads and networkequation.4.3.38) we easily get

$$\nabla H_n(\tilde{x}_n) = \nabla H_n(x_n) - \nabla H(x_n^*)$$

and, consequently,

$$\tilde{y}_n = g_n^T \nabla H_n(\tilde{x}_n) \tag{4.41}$$

Furthermore,

$$\dot{x}_n = \dot{\tilde{x}}_n = (J_n - R_n)\left(\nabla H_n(\tilde{x}_n) + \nabla H(x_n^*)\right) + g_n(\tilde{u}_n + u_n^*)$$

and the incremental dynamics of the system are given by,

$$\dot{\tilde{x}}_n = (J_n - R_n)\nabla H_n(\tilde{x}_n) + g_n \tilde{u}_n \tag{4.42}$$

Let u_n^* be the steady state value of the input u_n i.e. the desired current at the port (terminal) of generator where the generator is connected to the reminder of the system. For this value of u_n^* there is a corresponding steady state x_n^* of (4.39Passivity of inductive loads and networkequation.4.3.39) (for $v_n = 0$) given by,

$$x_n^* = M^{-1}(J_n - R_n)^{-1} g_n u_n^*$$

where the matrix $J_n - R_n$ is in the form

$$J_n - R_n = \begin{bmatrix} G & D & 0 & ..... & 0 \\ -D^T & R & 0 & ..... & 0 \\ 0 & 0 & (\omega_r N L_{load_1} - R_{load_1}) & ..... & 0 \\ 0 & 0 & 0 & . & 0 \\ 0 & 0 & 0 & . & 0 \\ 0 & 0 & 0 & ..... & (\omega_r N L_{load_{n_d}} - R_{load_{n_d}}) \end{bmatrix} \tag{4.43}$$

Here $D \in \mathbb{R}^{n_c} \times \mathbb{R}^{n_l}$, n_c the number of nodes and n_l the number of lines and n_d the number of loads. If for each load, $i \in 1, ..., n_d$, $R_{load_{n_d}} \neq 0$ and/or $L_{load_{n\,d}} \neq 0$ there is a unique nonzero solution for x_n^* associated with the generators terminal operating point that is scheduled by energy management control.

4.4 Generator Control

When we consider the synchronous generator system as a controlled system the field voltage v_f and the mechanical torque T_m are control inputs. In most "classical" applications the control objective is to regulate the terminal voltage, the generator frequency and the power output (real and reactive). The most common approach is to regulate the frequency and real power output is by adjusting the mechanical power (torque) input T_m (this requires a model of the prime mover that generates the mechanical torque). The terminal voltage and reactive power

are regulated by adjusting the field voltage.

For a fixed value of ω say $\omega = \omega_r$, and rotor phase angle $\triangle\theta_0$ define $A = A(\triangle\theta_0) = (N(\omega_R) - R\bar{L}^{-1}(\triangle\theta_0))$ and consider the steady state flux equation

$$0 = A\bar{\lambda}_s - \bar{v}_s$$

along with the design constraints

$$\begin{aligned} \bar{v}_{ts} &= \bar{v}_{td} \\ P_{es} &= \bar{i}_{ts}^T \bar{v}_{ts} = \bar{i}_s^T \bar{v}_s - i_{sf} v_{fs} = P_{ed} \\ Q_{es} &= \bar{i}_{ts}^T N \bar{v}_{ts} = Q_{ed} \end{aligned} \tag{4.44}$$

where $\bar{v}_{ts}$ is the terminal voltage part of $\bar{v}_s$, $\bar{\imath}_s = \bar{L}^{-1}(\Delta\theta_0)\bar{\lambda}_s$ and $\bar{v}_{td}$, P_{ed} and Q_{ed} are the design values for the terminal voltage and terminal real and reactive power. We can rewrite the steady state equations as

$$\begin{aligned} 0 = A(\triangle\theta_0)\bar{\lambda}_s - \bar{v}_s = A(\triangle\theta_0)\bar{L}(\triangle\theta_0)\bar{\imath}_s - \bar{v}_s \\ = A(\triangle\theta_0)\bar{L}(\triangle\theta_0) \begin{bmatrix} \bar{\imath}_{ts} \\ i_{fs} \end{bmatrix} - \begin{bmatrix} I \\ 0 \end{bmatrix} \bar{v}_{td} + \begin{bmatrix} 0 \\ 1 \end{bmatrix} v_{fs} \end{aligned} \tag{4.45}$$

Proposition 4.4.1. For given values of the steady state rotor speed and phase angle, $\omega = \omega_r$, $\triangle\theta = \triangle\theta_0$, as well as terminal voltage, $\bar{v}_{ts} = \bar{v}_{td}$, and terminal real and reactive powers, $P_{es} = P_{ed}$, $Q_{es} = Q_{ed}$ there exists a (unique upto phase shift) steady terminal current, $\bar{\imath}_{ts}$, and field voltage input v_{fs}. The steady state generator flux is given by $\bar{\lambda}_s = \bar{L}(\triangle\theta_0) \begin{bmatrix} \bar{\imath}_{ts} \\ i_{fs} \end{bmatrix}$ where $i_{fs} = \frac{v_{fs}}{R_f}$.

Proof. From the power design constraints and the terminal voltage constraint we can (completely) characterize $\bar{\imath}_{ts}$. Indeed, the steady state terminal voltage has the form $\bar{v}_{td}^T = \begin{bmatrix} V\cos\varphi_v & V\sin\varphi_v & 0 \end{bmatrix}$ and, similarly, the steady state terminal current has the form $\bar{\imath}_{ts}^T = \begin{bmatrix} I\cos\varphi_i & I\sin\varphi_i & 0 \end{bmatrix}$ for some I and φ_i.

From (4.44Generator Controlequation.4.4.44) we get $P_{ed} = VI\cos(\varphi_i - \varphi_v)$ and $Q_{ed} = VI\sin(\varphi_i - \varphi_v)$ and thus we see that we can solve for the unknown I and φ_i. Consider the equation (4.10equation.4.1.10) in steady state i.e.

$$0 = (J(\omega_r) - R)\nabla H(\bar{\lambda}) + m(\omega_r, \triangle\theta_0)i_f - \bar{v}$$

Noting that $J(\omega_r) - R = \begin{bmatrix} \omega_r(L_s + M_s)N - R_sI & 0 \\ 0 & -R_f \end{bmatrix}$ and $\nabla H(\bar{\lambda}_s) = \bar{\imath}_s$ we easily get

$$\begin{aligned} 0 &= (\omega_r(L_s + M_s)N - R_sI)\,\bar{\imath}_{ts} + \hat{m}(\omega_r, \triangle\theta_0)i_{fs} - \bar{v}_{ts} \\ 0 &= -R_f i_{fs} + v_{fs} \end{aligned}$$

where $\hat{m}(\omega_r, \triangle\theta_0)$ are the first three rows of $m(\omega_r, \triangle\theta_0)$. In the first equation everything is known except i_{fs} and the second equation uniquely relates i_{fs} and v_{fs}. Multiplying the first equation by $\hat{m}^T(\omega_r, \triangle\theta_0)$ on the left gives

$$i_{fs} = \frac{\hat{m}^T(\omega_r, \triangle\theta_0)\left(\bar{v}_{ts} - (\omega_r(L_s + M_s)N - R_sI)\,\bar{\imath}_{ts}\right)}{\frac{3}{2}M_f^2}.$$

We finally note that the steady state flux is given by $\bar{\lambda}_s = \bar{L}(\triangle\theta_0)\bar{\imath}_s$ where $\triangle\theta_0 = \theta_R - \theta_d$ is the steady state angle. □

The control problem can now be formulated as the problem of regulating the state $\bar{\lambda}$ to the steady state value $\bar{\lambda}_s$ and the rotor speed and angle to the design values $\omega_r, \triangle\theta_0$.

Consider the overall dynamics of the system on the form

$$\begin{aligned} \frac{d}{dt}\bar{\lambda} &= \left(N(\omega_r) - R\bar{L}^{-1}(\triangle\theta)\right)\bar{\lambda} - \bar{v} \\ \frac{d\triangle\theta}{dt} &= \triangle\omega \\ \frac{d}{dt}\triangle\omega &= \frac{1}{\bar{J}}\left(T_m - \frac{P_e}{\omega_r + \triangle\omega}\right) \end{aligned} \tag{4.46}$$

Linearizing (4.46Generator Controlequation.4.4.46) around the equilibrium point given by 4.44Generator Controlequation.4.4.44 gives

$$\frac{d}{dt}x = Fx + Gu + Hd$$

where

$$F = \begin{bmatrix} A(\triangle\theta_0) & Rl(\triangle\theta_0, \bar{\lambda}_s) & 0 \\ 0 & 0 & 1 \\ -\frac{a(\bar{v}_{ts}, \triangle\theta_0)}{\bar{J}} & -\frac{b(\bar{v}_{ts}, \triangle\theta_0, \bar{\lambda}_s)}{\bar{J}} & -\frac{c(\bar{v}_{ts}, \triangle\theta_0, \bar{\lambda}_s)}{\bar{J}} \end{bmatrix}$$

$$G = \begin{bmatrix} \begin{bmatrix} 0 \\ 1 \end{bmatrix} & 0 \\ 0 & 0 \\ 0 & 1 \end{bmatrix}, \; H = \begin{bmatrix} I \\ 0 \\ 0 \\ -\frac{d(\bar{v}_{ts},)}{\bar{J}}\triangle\theta_0 \end{bmatrix}$$

$$x = \begin{bmatrix} \triangle\bar{\lambda} \\ \delta\theta \\ \triangle\omega \end{bmatrix} = \begin{bmatrix} \triangle\bar{\lambda} \\ \triangle\theta - \triangle\theta_0 \\ \triangle\omega \end{bmatrix}$$

where the control input is input is $u = \begin{bmatrix} \triangle v_f \\ \triangle T \end{bmatrix}$ while $d = \triangle\bar{v}_t$ is a disturbance input and

$$\begin{aligned} \delta\theta &= (\triangle\theta - \triangle\theta_0) \\ \triangle T &= T_m - T_{es}, \\ a(\bar{v}_{ts}, \triangle\theta_0) &= \frac{\bar{v}_{ts}^T \begin{bmatrix} I & 0 \end{bmatrix} \bar{L}^{-1}(\triangle\theta_0)}{\omega_r} \\ b(\bar{v}_{ts}, \triangle\theta_0, \bar{\lambda}_s) &= \frac{\bar{v}_{ts}^T \begin{bmatrix} I & 0 \end{bmatrix} l(\triangle\theta_0, \bar{\lambda}_s)}{\omega_r} \\ c(\bar{v}_{ts}, \triangle\theta_0, \bar{\lambda}_s) &= -\frac{P_{ed}}{\omega_r} \\ d(\bar{\lambda}_s, \triangle\theta_0) &= \frac{\bar{\lambda}_s^T \bar{L}^{-1}(\triangle\theta_0) \begin{bmatrix} I \\ 0 \end{bmatrix}}{\omega_r} \end{aligned}$$

where $l(\triangle\theta_0, \bar{\lambda}_s) = -\bar{L}^{-1}(\triangle\theta_0)\frac{\partial\bar{L}(\triangle\theta_0)}{\partial\triangle\theta}\bar{L}^{-1}(\triangle\theta_0)\bar{\lambda}_s$.

The equilibrium point of the linearized system is at the origin, i.e. when $x = 0$ we have $\bar{\lambda} = \bar{\lambda}_s$ and $\omega = \omega_R$. We note that when $u = 0$ we have $T_{es} = T_m$.

The control objective is to regulate the state to zero for all values of the disturbance input. If we apply a state feedback law $u = -Kx$ to this system we get the closed loop system

$$\frac{d}{dt}x = (F - GK)x + Hd$$

Applying the Laplace transform to this equation we obtain

$$x(s) = (sI - (F - GK))^{-1}Hd(s) = (sI - (F - GK))^{-1}Hd(s)$$

Clearly, in order to reject the disturbance input d the feedback matrix K should be chosen so that the effect of the d on x is minimized, i.e. $G_{dx}(s, K) = (sI - (F - GK))^{-1}H$ should be "small". The first component of the control law is

$$\begin{aligned} \triangle v_f(s) &= \left[\begin{array}{cc} 1 & 0 \end{array}\right] u(s) = -\left[\begin{array}{cc} 1 & 0 \end{array}\right] Kx(s) \\ &= -\left[\begin{array}{cc} 1 & 0 \end{array}\right] KG_{dx}(s, K)d(s) \\ &= C(s)d(s) \end{aligned}$$

This control law has the familiar form $\triangle v_f(s) = C(s)d(s) = C(s)\left(\bar{v}_t - \bar{v}_{td}\right)$, i.e. exciter control where the objective is to select the exciter control input so as to regulate the terminal voltage to the zero. Since the terminal voltage is not a state in the generator system but rather an external input we see that the exciter control attempts to reject deviations of the terminal voltage from the steady state reference value.

The second component of the control law has the form

$$\begin{aligned} \triangle T &= \left[\begin{array}{cc} 0 & 1 \end{array}\right] u(s) = -\left[\begin{array}{cc} 0 & 1 \end{array}\right] Kx(s) \\ &= -\left[\begin{array}{cc} 0 & 1 \end{array}\right] KG_{dx}(s, K)d(s) = D(s)d(s) \end{aligned}$$

Consequently, deviations in the terminal voltage will result in deviations in the net torque and thus the terminal power output. We note that if K is chosen so

that $G_{dx}(j\omega, K)$) is small at all frequencies of interest the effect of variations in the terminal voltage on the generator output (i.e. real and reactive power) is reduced.

As we discussed in Section 5.4Dynamics and Stability of Interconnected Power System Componentssection.5.4 the stability of the overall power system depends on the interconnection of the system components. This is a well studied problem for the swing dynamics of interconnected generators and various stability conditions exists for synchronous operation. Stability conditions for systems where the time scale separation between the swing and electrical dynamics is no longer valid has been limited to linear analysis [46]. A notable exception is [15] where a full nonlinear synchronous generator connected to a simple load was considered and clearly this is an open area of research.

In this section we discussed how control laws should be designed to minimize the effect of small variations in the terminal conditions of a synchronous generator, i.e. local control that does not have access or knowledge to a model of the rest of the system.

4.5 Summary

In this chapter, we reviewed dynamical systems modeling and control in sense of energy. Port-Hamiltonian systems as a class of energy based systems that can be applied to model power system's components in a unified approach is reviewed. Interconnection and Damping Assignment Control as a passivity-based control method for port-Hamiltonian systems is discussed.

Chapter 5

Modeling and Control of Inverter-based Generators

A disadvantage of integrating renewable energy into power systems is the very short-term electrical storage in power electronic devices applied at their interface with the grid. Therefore, frequency spikes resulting from transient power unbalances and other incidences in the grid can be considerable. Lack of inertia when integrating renewable energy into power systems, might cause stability problems. As the size of generation units that are based on renewable energy resources is often considerably smaller than conventional synchronous generators, their impact on transient stability of power systems in lower penetration levels can be neglected. However, when their share in power generation is considerable, their dynamic behavior affects the stability of the whole system [52].

Slootweg and Kling in [52] investigate the impact of various DG technologies and their penetration level in transient stability of power systems. High penetration of DGs based on power electronic devices results in large voltage drops at some nodes after occurrence of a fault. The conventional inverter design neglects the power quality and is based on transmitting the maximum energy into the grid. Therefore, to insure the desired voltage profile, a reliable controller is required.

There are various control algorithms for inverters at lower or higher orders that mimic synchronous machines characteristics and whose goal is to help stability

of the system by introducing inertia, damping and other dynamic characteristics. These control algorithms are the basis for Virtual Synchronous Machines (VSM) [3]. VSM techniques establish the static and dynamic performance of synchronous generators. Applying these algorithms, despite lack of any actual physical mass of inertia, the generation units fed by renewable energy resources emulate power response of a real synchronous generator. Virtual torque and excitation circuit in VSM enable the grid connected inverters to regulate active and reactive power.

An inverter is a power electronic device that generates AC voltage or current from a DC input by operating switches. The switches are controlled by a controller that receives as input the frequency and amplitude of the desired inverter output AC waveform. Consequently, from a higher level control perspective, the inverter is an actuator that receives an input reference waveform and generates an output that traces the input waveform. The inverter power electronics controller and switches operate at a frequency that is much higher than the frequency of the output waveform.

The inverter output waveform is generally speaking a piecewise continuous waveform that approximates the ideal sinusoidal reference signal and even after notch filtering has a considerably high frequency content that may affect system stability. This issue is not addressed in this dissertation. We will view the inverter with its power electronic controller as an ideal voltage or current source whose frequency and magnitude can be controlled. As stated previously, it is desired to operate this ideal source so as to mimic some of the behavior of a synchronous generator when the source is connected to the grid. In order to react to changes (in voltage, frequency, active power and reactive power) at the terminal of the inverter a controller is built that generates the reference frequency and magnitude.

The simplest such model adjusts the frequency and magnitude using a decoupled first order models for the frequency and magnitude variations. This control approach is frequently called droop control. A more sophisticated approach is based on mimicking the response of a synchronous generator. In particular, a model that is driven by the terminal voltage and mimic the flux dynamics of a synchronous machine is built and the output of this model generates the reference current for the inverter. This control approach is often called a Virtual Synchronous Machine (VSM) or Synchronverter. Several various of this approach have been suggested in the literature and are of various degrees of complexity. In section 5.1Droop Controlsection.5.1 and section 5.2Virtual Synchronous Machinessection.5.2 we review these approaches.

In this dissertation we formulated a novel VSM approach based on a port-Hamiltonian formulation. We mimic all dynamic behavior of the synchronous machine to the first order (i.e. by linear model close to a scheduled slowly varying operating point). Due to the fact that the model is based on port-Hamiltonian formulation it has the potential of accounting for fast electric transients and disturbances at the interface of the inverter and the rest of the system.

5.1 Droop Control

The control objective of power sharing is to specify the desired steady-state sharing of the power demand among generation units [51]. Droop control technique is a decentralized proportional control based on power-speed characteristic of synchronous generators is widely used to direct active power sharing in power systems with large scale fossil fuel based conventional generation units. Droop control has been a common method for regulating active and reactive power in microgrids

with inverter-based generation units. In a microgrid with several parallel-connected inverter-based generator units, voltage and frequency droop control is a popular method to control the share of power that is delivered by each unit [37, 54]. In an inductive system the active and reactive power of each generation unit is

$$P = \frac{EVsin\delta}{X} \tag{5.1}$$

$$Q = \frac{EVcos\delta - V^2}{X} \tag{5.2}$$

where E is the inverter terminal voltage amplitude, V is the common bus voltage amplitude, δ is the power angle and X is the output reactance of the inverter. As we can see in (5.1Droop Controlequation.5.1.1) and (5.2Droop Controlequation.5.1.2), a network model of a micro-grid with purely inductive lines i.e. $\delta \approx 0$, active power flows are mainly functions of frequency and reactive power flows are functions of voltage magnitudes. Active power droop control and reactive power droop control are proportional controllers for controlling frequency and voltage magnitude, respectively.

Active power droop control builds a relation between active power and frequency that is very similar to the swing equation of synchronous generators [23],

$$\Delta\dot{\omega} = -d\Delta\omega - k_P(P - P_d) \tag{5.3}$$

where $\Delta\omega = \omega - \omega_d$, d is a damping ratio and ω_d (typically $\omega_d = \omega_r$) and P_d are the desired values of frequency and active power, respectively. Reactive power droop control is a proportional controller that relates reactive power flows and voltage magnitudes [23],

$$\Delta\dot{V} = -d\Delta V - k_Q(Q - Q_d) \tag{5.4}$$

where $\Delta V = V - V_d$, V_d and Q_d are the desired values of voltage magnitude and reactive power, respectively. The gains k_p and k_Q should be selected to satisfy the operational criteria such as control loop bandwidth and stability [35]. In systems with considerable line resistance, the original droop control in (5.3Droop Controlequation.5.1.3)-(5.4Droop Controlequation.5.1.4) does not produce satisfactory results. Several modified droop control strategies have been suggested to address this issue [5], [36].

Droop control techniques are considered as a lower-level VSM algorithm that corresponds to swing ewuation of a synchronous generator [3, 12, 13, 24]. Another group of techniques to control and operate inverter-based microgrids that are based on emulating the electromagnetic equations of synchronous generators are reviewed next.

5.2 Virtual Synchronous Machines

This control technique is based on emulating the essential properties of a conventional synchronous generator such as inertia and damping to provide simplicity in operating inverter-based generation units. The mathematical model of synchronous generators consists of two set of equations that describe its mechanical (swing equation) and electrical (the stator and rotor winding equations) parts. The higher order model of synchronous generators is applied to calculate the reference values for either virtual stator current or voltage. As explained above, VSM is a controller that is added to the inverter switching controller to enable it to behave as a synchronous generator [3]. The functions in controlling an inverter-based generator can be expressed in three tasks:

1 To feed the VSM algorithm with voltage/current and frequency measurements.

2 To perform VSM algorithm i.e applying the mathematical equations that are emulating electrical and mechanical performance of a synchronous generator and calculate a reference voltage (current) for CSI (VSI) in real time.

3 Employing the calculated reference values for generating the proper pulses to trigger power electronic circuit of the inverter.

Zhong and Weiss in [58] introduce the dynamics and operation of synchronverters based on synchronous genrators dynamics and apply frequency- and voltage-drooping mechanisms to share active and reactive power among parallel connected synchronverters. The approach in [58] is based on the full synchronous generator model equations (4.10equation.4.1.10)-(4.11equation.4.1.11). However, they make certain steady state simplifications that result in voltage source model, i.e. an equation of the form (4.14equation.4.1.14) for the electrical part of the inverter model. The inertial model for the frequency dyncamics of the inverter model is a full dynamic model mimicing a synchronous generator rotational dynamics. Alsiraji and El-Shatshat in [3] call the control algorithms that emulates the properties of traditional synchronous machines, Virtual synchronous machine (VSM) and categorize these methods into high and low order models. The low-order VSM models are based on swing equation and similar to the conventional droop control [12].

Fig 2.2DC-AC voltage conversion by an inverter [21]. (Reprinted with permission)figure.2.2 illustrates a typical inverter-based distributed generation unit that consists of an energy source unit that converts renewable energy to DC form

of electricity, a capacitor bank to stabilize the DC link voltage, an inverter that converts electricity to AC form with the network frequency and an filter to remove the high frequency contents.

These VSM techniques are basically divided in two categories:

- Current Source Inverter (CSI)- In this methods the grid voltage is measured and virtual synchronus machine algorithm calculates the refenrece current for the pulse generating unit [6, 8, 9].
- Voltage Source Inverter (VSI)- In this methods the pulse generating unit is fed by the reference voltage that is calculated using the measured phase currents [4, 48, 57, 58].

The pulse generating unit that uses these reference signals typically uses either a hysteresis current control technique (in CSI) or PWM control technique (in VSI) or extensions/alternatives of these techniques [10]. The choice of modulation technique affects the Total Harmonic Distortion (THD) of the inverter output [25].

5.2.1 Average Modeling

Modeling of microgrids components to simulate their nonlinearity in reasonable computing time is required for stable operation and accurate analysis of microgrids. Therefore, complete and detailed switching models for power electronic systems are not practical in operation and analysis of microgrids and time-efficient models with enough accuracy are needed for this purposes.

As in Fig. 5.1A typical 2-level 3-phase structure of inverter-based generator in a microgrid [25]. (Copyright 2014, IEEE)figure.5.1, a voltage source inverter, is

connected to a low pass filter that consists of an inductor L_1 and a capacitor bank C_f. Inductor L_2 represents the leakage inductance of the microgrid side isolation transformer and isolates the inverter-based generator from the microgrid. Average modeling involves representing the output voltage (current) at point of common coupling as average waveform.

Space Vector Modulation (SVM) [25] is applied to generate gate signals for the inverter's switches. In a commonly used 2-level 3-phase inverter Fig. 5.1A typical 2-level 3-phase structure of inverter-based generator in a microgrid [25]. (Copyright 2014, IEEE)figure.5.1, the pole voltages are $\frac{V_{dc}}{2}$ and $\frac{-V_{dc}}{2}$ and there are 2^3 switching states where two of these switching states are null states (represents zero volts at the terminal) and the rest are active states. SVM is used to produce the switches gate signals. Fig. 5.2SVM diagram of 2-level 3-phase Voltage Source Inverter [30]. (Copyright 2017, IEEE)figure.5.2 shows the corresponding vectors of these eight states. The null states ($(000)V_0$ and $(111)V_7$) have zero value and are located at the origin. Vectors with 180° angle difference, are corresponding with the same phase, i.e. $(100)V_1$ and $(011)V_4$ represent phase a, $(110)V_2$ and $(001)V_5$ represent phase b and $(101)V_6$ and $(010)V_3$ represent phase c. Any voltage vector can be synthesized by altering between to adjacent states e.g. V_{ref} in Fig. 5.2SVM diagram of 2-level 3-phase Voltage Source Inverter [30]. (Copyright 2017, IEEE)figure.5.2 is located between V_1 and V_2. As Fig. 5.3V_{ref} is transformed into on/off signals for switches by a triangular wave (T_s is the switching period.) [30]. (Copyright 2017, IEEE)figure.5.3 shows voltage V_{ref} can be transformed into on/off signals for each leg in each phase by using a triangular triggering wave. Note that different approaches in distributions of null state times T_0 and T_7 result in different SVM types.

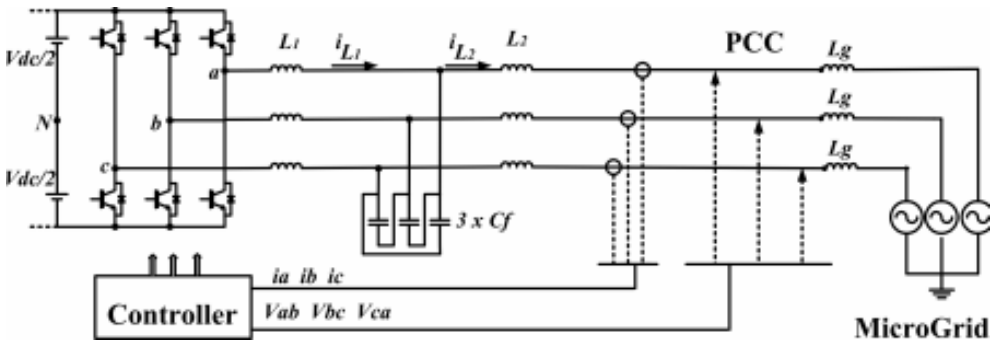

Figure 5.1: A typical 2-level 3-phase structure of inverter-based generator in a microgrid [25]. (Copyright 2014, IEEE)

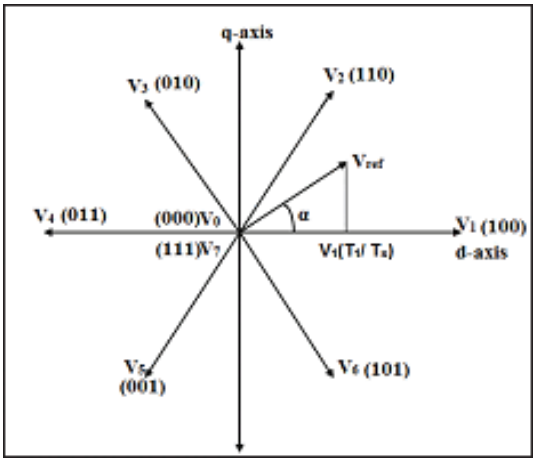

Figure 5.2: SVM diagram of 2-level 3-phase Voltage Source Inverter [30]. (Copyright 2017, IEEE)

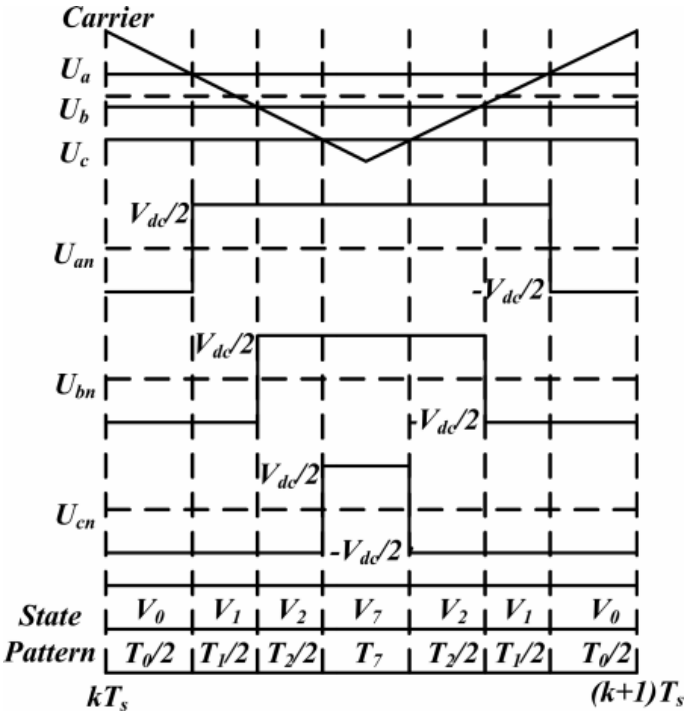

Figure 5.3: V_{ref} is transformed into on/off signals for switches by a triangular wave (T_s is the switching period.) [30]. (Copyright 2017, IEEE)

5.3 Proposed Technique for Modeling and Control of Inverter-based Generator

In this section, a port-Hamiltonian model of an inverter-based generator is proposed where the port variables are the terminal voltage (input) and current (output) produced by the generator. The suggested model is inspired by the synchronous generator equations and two sets of dynamical equations are introduced for inverter-based generator model that are motivated by the corresponding equations of a synchronous generator.

We express the inverter-based generator model around the (desired) equilibrium point.

5.3.1 Generator Model For Current Source Inverter (CSI)

Consider a Hamiltonian function of the form,

$$H_{Inv}(X_e, \Delta\omega, \Delta\theta) = \frac{1}{2}(X_e - X_{e_s})^T \Gamma^{-1}(\Delta\theta)(X_e - X_{e_s}) + \frac{1}{2}\Delta\omega^2 \tag{5.5}$$

where X_e, $\Delta\omega$ and $\Delta\theta$ are the states and $\Gamma(\Delta\theta)$ is an operator matrix. Here X_{es} is an equilibrium state that is derived for a desired operating point of the generator (e.g. for a scheduled real and reactive power as well as nominal terminal voltage). The state X_e is related to the terminal currents and an "internal current" through the relationship,

$$X_e = \begin{bmatrix} X_{e_d} \\ X_{e_q} \\ X_{e_f} \end{bmatrix} = \Gamma(\Delta\theta) \begin{bmatrix} i_d \\ i_q \\ i_f \end{bmatrix} = \begin{bmatrix} L1 & 0 & L_3 \\ 0 & L1 & L_3\Delta\theta \\ L_3 & L_3\Delta\theta & L_2 \end{bmatrix} \begin{bmatrix} i_d \\ i_q \\ i_f \end{bmatrix} \tag{5.6}$$

Here i_d and i_q are the terminal currents in dq reference frame and i_f is an "internal current" that is essentially a control variable. We note that we have dropped the "0" currents in the $dq0$ formulation and assume that balanced conditions

where the "0" current is identically zero is valid. Note that $X_e = \Gamma(\Delta\theta)i$, where $\Gamma(\Delta\theta) = \Gamma_0 + \Gamma_1\Delta\theta$, $i = \begin{bmatrix} i_t & i_f \end{bmatrix}^T = \begin{bmatrix} i_d & i_q & i_f \end{bmatrix}^T$

$$\Gamma_0 = \begin{bmatrix} L_1 & 0 & L_3 \\ 0 & L_1 & 0 \\ L_3 & 0 & L_2 \end{bmatrix} \quad \text{and} \quad \Gamma_1 = \begin{bmatrix} 0 & 0 & 0 \\ 0 & 0 & L_3 \\ 0 & L_3 & 0 \end{bmatrix}.$$

$\Delta\omega$ is deviation of the inverter frequency from the system frequency ω_r. The last element in the state vector X_e, i.e. X_{e_f}, corresponds to the so-called excitation circuit in synchronous generator and is a control variable.

If we define $\tilde{X}_e = X_e - X_{e_s}$ we can write the Hamiltonian function as,

$$H_{Inv} = \frac{1}{2}\begin{bmatrix} \tilde{X}_e^T & \Delta\omega & \Delta\theta \end{bmatrix} \begin{bmatrix} \Gamma^{-1}(\Delta\theta) & 0 & 0 \\ 0 & 1 & 0 \\ 0 & 0 & 0 \end{bmatrix} \begin{bmatrix} \tilde{X}_e \\ \Delta\omega \\ \Delta\theta \end{bmatrix} \tag{5.7}$$

The gradient of Hamiltonian function has the form,

$$\nabla H_{inv} = \begin{bmatrix} \Gamma^{-1}(\Delta\theta)\tilde{X}_e \\ \Delta\omega \\ -\frac{1}{2}\tilde{i}^T\Gamma_1\tilde{i} \end{bmatrix} = \begin{bmatrix} \tilde{i} \\ \Delta\omega \\ -\tilde{i}_f\tilde{i}_q L_3 \end{bmatrix} \tag{5.8}$$

where $\tilde{i} = i - \bar{i}$, $\bar{i}$ is the current vector at the equilibrium point,

$$\bar{i} = \begin{bmatrix} i_{d_s} & i_{q_s} & i_{f_s} \end{bmatrix}^T$$

The dynamic equations for the port-Hamiltonian inverter model are chosen as,

$$\begin{bmatrix} \dot{\tilde{X}}_e \\ \Delta\dot{\omega} \\ \Delta\dot{\theta} \end{bmatrix} = (J_{inv} - R_{inv})\nabla H_{inv} + g_{inv} \begin{bmatrix} v_t - \bar{v}_t \\ u_f - u_{f_s} \\ u_p - u_{p_s} \end{bmatrix} \tag{5.9}$$

where v_t is the terminal voltage, $g_{inv} = \begin{bmatrix} -I & 0 \\ 0 & 1 \\ 0 & 0 \end{bmatrix}$, the skew-symmetric interconnection matrix is defined as,

$$J_{inv} = \begin{bmatrix} 0 & -\omega_r L_1 & 0 & -v_{d_s} & 0 \\ \omega_r L_1 & 0 & \frac{\omega_r L_3}{2} & -v_{q_s} & 0 \\ 0 & -\frac{\omega_r L_3}{2} & 0 & -u_{f_s} & 0 \\ v_{d_s} & v_{q_s} & u_{f_s} & 0 & -1 \\ 0 & 0 & 0 & 1 & 0 \end{bmatrix}$$

and the symmetric positive-semi definite dissipation matrix is,

$$R_{inv} = \begin{bmatrix} R_1 & 0 & 0 & 0 & 0 \\ 0 & R_1 & -\frac{\omega_r L_3}{2} & 0 & 0 \\ 0 & -\frac{\omega_r L_3}{2} & R_2 & 0 & 0 \\ 0 & 0 & 0 & d & 0 \\ 0 & 0 & 0 & 0 & 0 \end{bmatrix}$$

Here, L_1, L_2, L_3, R_1 are the model coefficients and v_{d_s}, v_{q_s}, u_{f_s} are the elements of the terminal voltage vector $\bar{v}_t$ and the control "voltage", u_f at the desired equilibrium point. We note that the control input u_p and its steady state value u_{p_s} correspond to the torque input in the synchronous generator. Furthermore, the terminal input variable in (5.15Generator Model For Voltage Source Inverter (VSI)equation.5.3.15) is the voltage and the output variable is the current $\begin{bmatrix} i_t - \bar{i}_t \\ i_f - \bar{i}_f \end{bmatrix} = \nabla H_{Inv}(\tilde{X}_e, \Delta\omega, \Delta\theta)$.

The dissipation matrix, R_{inv} is positive-semi definite provided the following condition holds,

$$R_1 R_2 \geq (\frac{\omega_r L_3}{2})^2 \tag{5.10}$$

We assume this condition is satisfied throughout this dissertation.

5.3.2 Generator Model For Voltage Source Inverter (VSI)

For Voltage Source Inverter, we construct a control law model that is based on a linearization of electrostatic generator model in example 4.1.5exmp.4.1.5. In particular, linearizing the generator equations around a given operating point (4.15equation.4.1.15) results in a system with Hamiltonian function of the form

$$H_{Inv}(X_g, \Delta\omega, \Delta\theta) = \frac{1}{2}(X_g - X_{g_s})^T \Lambda^{-1}(\Delta\theta)(X_g - X_{g_s}) + \frac{1}{2}\Delta\omega^2 \tag{5.11}$$

where X_g, $\Delta\omega$ and $\Delta\theta$ are the states and $\Lambda(\Delta\theta)$ is an operator matrix. Here X_{gs} is an equilibrium state obtained from the desired operating point. The state X_g is

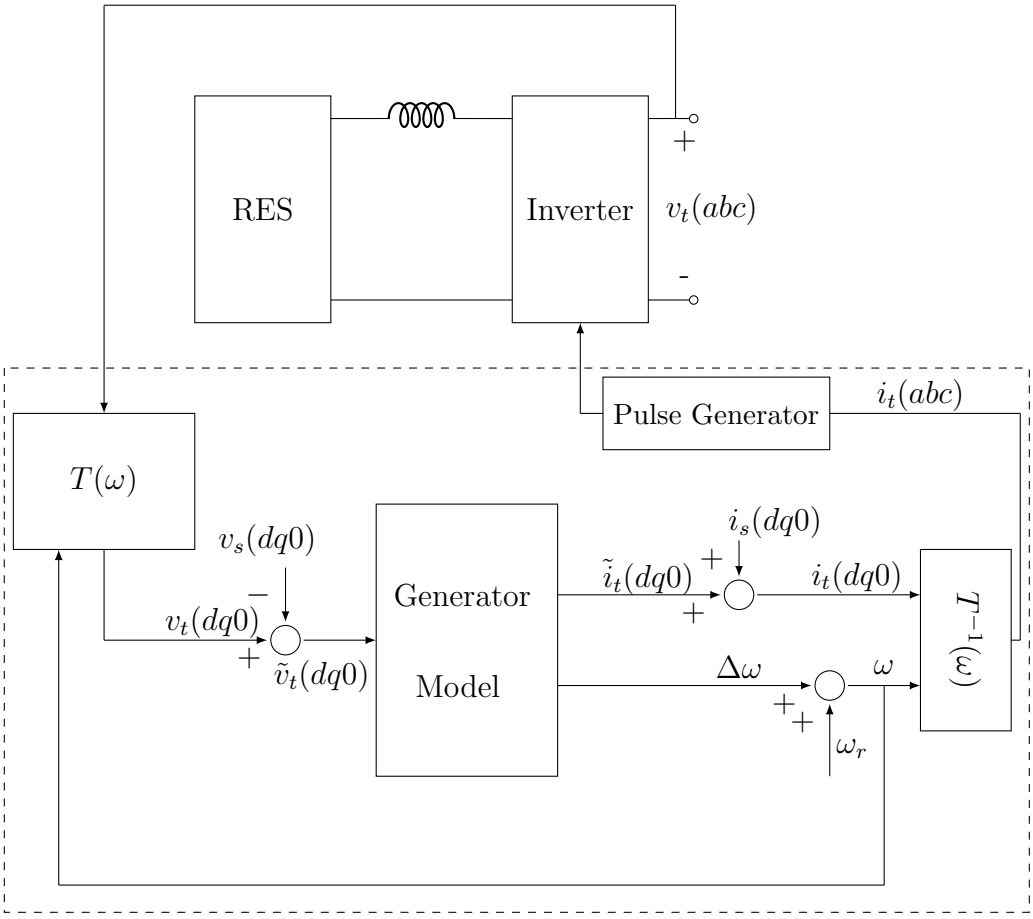

Figure 5.4: Schematic diagram of the open loop inverter-based generator design.

related to the terminal voltages and an "internal voltage" through the relationship

$$X_g = \begin{bmatrix} X_{g_d} \\ X_{g_q} \\ X_{g_f} \end{bmatrix} = \Lambda(\Delta\theta) \begin{bmatrix} v_d \\ v_q \\ v_f \end{bmatrix} = \begin{bmatrix} \lambda_1 & 0 & \lambda_3 \\ 0 & \lambda_1 & \lambda_3\Delta\theta \\ \lambda_3 & \lambda_3\Delta\theta & \lambda_2 \end{bmatrix} \begin{bmatrix} v_d \\ v_q \\ v_f \end{bmatrix} \tag{5.12}$$

Here v_d and v_q are the terminal voltages in dq reference frame and v_f is an "internal voltage" that is essentially a control variable. Note that $X_g = \Lambda(\Delta\theta)v$, where $\Lambda(\Delta\theta) = \Lambda_0 + \Lambda_1\Delta\theta$, $v = \begin{bmatrix} v_t & v_f \end{bmatrix}^T = \begin{bmatrix} v_d & v_q & v_f \end{bmatrix}^T$

$$\Lambda_0 = \begin{bmatrix} \lambda_1 & 0 & \lambda_3 \\ 0 & \lambda_1 & 0 \\ \lambda_3 & 0 & \lambda_2 \end{bmatrix} \quad \text{and} \quad \Lambda_1 = \begin{bmatrix} 0 & 0 & 0 \\ 0 & 0 & \lambda_3 \\ 0 & \lambda_3 & 0 \end{bmatrix}.$$

$\Delta\omega$ is deviation of the inverter frequency from the system frequency ω_r. The last element in the state vector X_g, i.e. X_{g_f} is a control variable.

If we define $\tilde{X}_g = X_g - X_{g_s}$ we can write the Hamiltonian function as,

$$H_{Inv} = \frac{1}{2} \begin{bmatrix} \tilde{X}_g^T & \Delta\omega & \Delta\theta \end{bmatrix} \begin{bmatrix} \Lambda^{-1}(\Delta\theta) & 0 & 0 \\ 0 & 1 & 0 \\ 0 & 0 & 0 \end{bmatrix} \begin{bmatrix} \tilde{X}_g \\ \Delta\omega \\ \Delta\theta \end{bmatrix} \tag{5.13}$$

The gradient of Hamiltonian function has the form,

$$\nabla H_{inv} = \begin{bmatrix} \Lambda^{-1}(\Delta\theta)\tilde{X}_g \\ \Delta\omega \\ -\frac{1}{2}\tilde{v}^T\Lambda_1\tilde{v} \end{bmatrix} = \begin{bmatrix} \tilde{v} \\ \Delta\omega \\ -\tilde{v}_f\tilde{v}_q\lambda_3 \end{bmatrix} \tag{5.14}$$

where $\tilde{v} = v - \bar{v}$, $\bar{v}$ is the voltage vector at the equilibrium point,

$$\bar{v} = \begin{bmatrix} v_{d_s} & v_{q_s} & v_{f_s} \end{bmatrix}^T$$

The dynamic equations for the port-Hamiltonian inverter model are give by,

$$\begin{bmatrix} \dot{\tilde{X}}_g \\ \Delta\dot{\omega} \\ \Delta\dot{\theta} \end{bmatrix} = (J_{inv} - R_{inv})\nabla H_{inv} + g_{inv} \begin{bmatrix} \tilde{i}_t \\ \tilde{i}_f \\ \tilde{u}_q \end{bmatrix} \tag{5.15}$$

where $\tilde{i}_t = i_t - \bar{i}_t$, $\tilde{i}_f = i_f - i_{f_s}$, $\tilde{u}_q = u_q - u_{q_s}$, i_t is the terminal current, $g_{inv} = \begin{bmatrix} -I & 0 \\ 0 & 1 \\ 0 & 0 \end{bmatrix}$, the skew-symmetric interconnection matrix is defined as,

$$J_{inv} = \begin{bmatrix} 0 & -\omega_r\lambda_1 & 0 & -i_{d_s} & 0 \\ \omega_r\lambda_1 & 0 & \frac{\omega_r\lambda_3}{2} & -i_{q_s} & 0 \\ 0 & -\frac{\omega_r\lambda_3}{2} & 0 & -i_{f_s} & 0 \\ i_{d_s} & i_{q_s} & i_{f_s} & 0 & -1 \\ 0 & 0 & 0 & 1 & 0 \end{bmatrix}$$

and the symmetric positive-semi definite dissipation matrix is,

$$R_{inv} = \begin{bmatrix} G_1 & 0 & 0 & 0 & 0 \\ 0 & G_1 & -\frac{\omega_r\lambda_3}{2} & 0 & 0 \\ 0 & -\frac{\omega_r\lambda_3}{2} & G_2 & 0 & 0 \\ 0 & 0 & 0 & d & 0 \\ 0 & 0 & 0 & 0 & 0 \end{bmatrix}$$

λ_1, λ_2, λ_3, G_1, G_2 and d are the model's coefficients and i_{d_s}, i_{q_s}, i_{f_s} are the elements of the current vector at the desired equilibrium point $\bar{i}_t$.

The dissipation matrix, R_{inv} is positive-semi definite provided the following condition holds,

$$G_1 G_2 \geq (\frac{\omega_r\lambda_3}{2})^2 \tag{5.16}$$

In (5.15Generator Model For Voltage Source Inverter (VSI)equation.5.3.15) $\tilde{i}_f$ and $\tilde{u}_q$ are control inputs that can be selected to regulate the frequency (voltage) and active and reactive power outputs. For a PWM based inverter as shown in Fig. 5.7Schematic diagram of the closed-loop inverter-based controllerfigure.5.7 the generator model in (5.15Generator Model For Voltage Source Inverter (VSI)equation.5.3.15) provides the reference value for the inverter PWM control algorithm. We note that the input to (5.15Generator Model For Voltage Source Inverter (VSI)equation.5.3.15) is the generator terminal current.

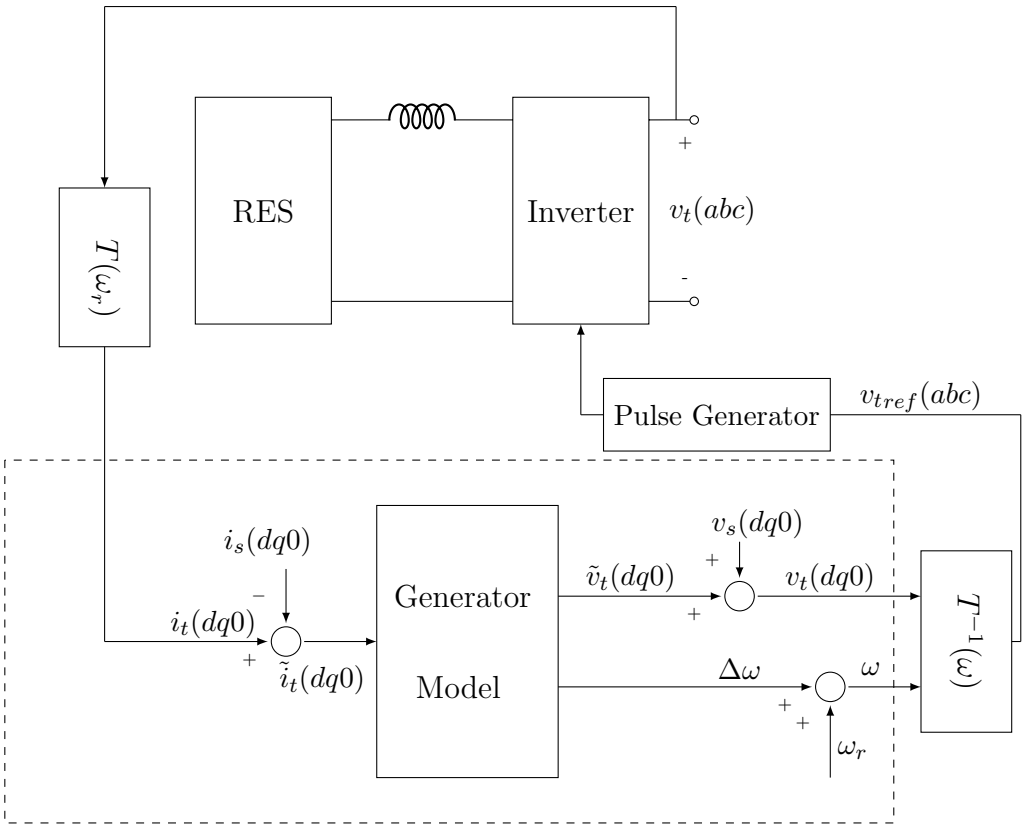

Figure 5.5: The proposed voltage source inverter-based controller.

5.4 Dynamics and Stability of Interconnected Power System Components

The Hamiltonian model of the electrical dynamics of a virtual CIS synchronous generator has the form,

$$\dot{\tilde{x}}_{Inv} = (J_{Inv} - R_{Inv})\nabla H_{Inv}(\tilde{x}_{Inv}) + g_{Inv}\bar{u} \tag{5.17}$$

$$y_{Inv} = \begin{bmatrix} -\tilde{i}_t \\ \tilde{i}_f \\ \Delta\omega \end{bmatrix}$$

where $\tilde{x}_{Inv} = \begin{bmatrix} \tilde{X}_e \\ \Delta\omega \\ \Delta\theta \end{bmatrix}$, $\bar{u} = \begin{bmatrix} \tilde{v}_t \\ \tilde{u}_f \\ \tilde{u}_p \end{bmatrix}$. The network and load that is connected to the generator can be represented by a total Hamiltonian function H_n that is typically a quadratic function of network and load inductance's fluxes and capacitance's charges,

$$\dot{x}_n = (J_n(x_n) - R_n(x_n))\nabla H_n(x_n) + g_n(x_n)u_n + e_n(x_n)v_n \tag{5.18}$$

$$y_n = g_n^T(x_n)\nabla H_n(x_n)$$

where $y_n = \tilde{v}_t$, $u_n = -\tilde{i}_t$ are the port variables and v_n is an external input. The system consisting of the synchronous generator and the network and load port-Hamiltonian model has the overall Hamiltonian function $H_t(x_g, x_n) = H_g(x_g) + H_n(x_n)$ and dynamic equations of the overall system is of the form,

$$\begin{bmatrix} \dot{x}_g \\ \dot{x}_n \end{bmatrix} = (J_t(x_g, x_n) - R_t)\nabla H_t(x_1, x_2) + g_t u_t + E(x_n)v_n \tag{5.19}$$

While each individual component H_{inv} and H_n may be a stable system in isolation, in general the interconnected system may not be stable for all the operating conditions and stability can only be achieved by an appropriate control design such as Interconnection and Damping Assignment (IDA) [41, 42] where a desired Hamiltonian function is assigned by proper control law design. This requires complete

knowledge of H_n which in reality mat not be available and thus alternative methods such as robust IDA may be needed. Such problem will be studied in future research. Below we present the IDA design for a simple microgrid system.

5.5 Control Design

To achieve overall system stability, we shape the energy of the system to a desired function that is positive semi-definite and whose time-derivative is non-positive for any initial condition. Interconnection and damping assignment disscussed in section 3.4.1Interconnection and Damping Assignment (IDA) Controlsubsection.3.4.1 provides a methodology for assigning the desired energy function and structure to the closed loop system [41]. The desired energy function has minimum value at the desired equilibrium point and the interconnection and damping matrices are assigned to provide the appropriate control law [41], [42]. Galaz, Ortega, et al. develope a passivity based control method for adjusting the behavior of a nonlinear system. In [16] this methodology is used to design the excitation control of synchronous generators.

For a simplified inverter-based microgrid consisting of single line, constant impedance load and single CSI inverter-based generator system described in section 5.3.1Generator Model For Current Source Inverter (CSI)subsection.5.3.1 (Fig.5.6The open loop system consisting of a Current Source Inverter (CSI), a line and a load, all modeled as port-Hamiltonian systemsfigure.5.6), the Hamiltonian function for the system connected to the CSI inverter-based generator can be expressed as the sum of two terms,

$$H_n = H_{line} + H_{load} \tag{5.20}$$

We write the Hamiltonian function of the overall system in the form,

$$H(x) = \frac{1}{2}(x - x_s)^T Q(x - x_s) \tag{5.21}$$

where x_s is the desired equilibrium point so $H(x)$ is minimum at x_s i.e. $\nabla H|_{x=x_s} = 0$. The port-Hamiltonian model of the system has the form,

$$\dot{\tilde{x}} = (\tilde{J} - \tilde{R})\nabla H(\tilde{x}) + g\tilde{u} \tag{5.22}$$

$$\tilde{u} = \begin{bmatrix} u_f - u_{f_s} \\ u_p - u_{p_s} \end{bmatrix}$$

where the Hamiltonian function is,

$$H(\tilde{x}) = \frac{1}{2}\tilde{x}^T Q(\Delta\theta)\tilde{x} \tag{5.23}$$

and

$$\tilde{R} = diag(R_{line}, R_{load}, R_{inv}),$$

$$\tilde{J} = \begin{bmatrix} J_{line} & I & B' \\ -I & J_{load} & 0 \\ -B'^T & 0 & J_{inv} \end{bmatrix},\ B' = \begin{bmatrix} I_{2\times 2} & 0_{2\times 2} \end{bmatrix},$$

$$Q(\Delta\theta) = \begin{bmatrix} K & 0 & 0 & 0 \\ 0 & \Gamma^{-1}(\Delta\theta) & 0 & 0 \\ 0 & 0 & 1 & 0 \\ 0 & 0 & 0 & 0 \end{bmatrix}$$

The above Hamiltonian function is minimum at x_s but matrix $Q(\Delta\theta)$ is not positive-semi definite. Indeed,

$$\frac{1}{2}X_e^T\Gamma^{-1}(\Delta\theta)X_e = \frac{1}{2}i^T\Gamma(\Delta\theta)i = \frac{1}{2}i^T(\Gamma_0 + \Gamma_1\Delta\theta)i$$

$$= \frac{1}{2}i^T\Gamma_0 i + \frac{1}{2}i^T\Gamma_1 i\Delta\theta$$

$$= \frac{1}{2}X_e^T\Gamma^{-1}(\Delta\theta)\Gamma_0\Gamma^{-1}(\Delta\theta)X_e + L_3 i_d i_q \Delta\theta$$

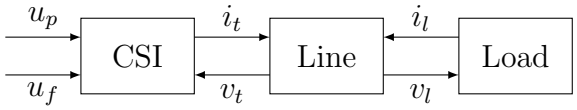

Figure 5.6: The open loop system consisting of a Current Source Inverter (CSI), a line and a load, all modeled as port-Hamiltonian systems.

$H(\tilde{x})$ can be rewritten as,

$$H(\tilde{x}) = \frac{1}{2}\tilde{x}^T Q_0(\Delta\theta)\tilde{x} + L_3\tilde{i}_f\tilde{i}_q\Delta\theta \tag{5.24}$$

For a π model line with node capacitance values of c_1 and c_2 and inductance value of l and an inductive load with inductance value of l_l,

$$Q_0(\Delta\theta) = \begin{bmatrix} K & 0 & 0 & 0 \\ 0 & \Gamma^{-1}(\Delta\theta)\Gamma_0\Gamma^{-1}(\Delta\theta) & 0 & 0 \\ 0 & 0 & 1 & 0 \\ 0 & 0 & 0 & 0 \end{bmatrix}$$

and K is the orthogonal matrix of load and line capacitance and inductance matrices:

$$K = diag(C_1^{-1}, C_2^{-1}, L^{-1}, L_l^{-1})$$

where $C_1 = c_1 I$, $C_2 = c_2 I$, $L = lI$, $L_l = l_l I$ (I is the identity matrix). For $L_1 \geq 0$ and $L_1 L_2 \geq L_3^2$, Q_0 is positive semi-definite. We assume this condition is true the reminder of this paper. Applying IDA methodology in section 3.4.1Interconnection and Damping Assignment (IDA) Controlsubsection.3.4.1 to the interconnected power system we choose the desired quadratic energy function H_d as,

$$H_d = \frac{1}{2}\tilde{x}^T Q(\Delta\theta)\tilde{x} + \frac{1}{L_1(L_1L_2 - L_3^2)}(L_3\tilde{X}_{e_d} - L_1\tilde{X}_{e_f})^2 +$$

$$\frac{1}{L_1}\tilde{X}_{e_q}^2 + \frac{1}{L_1L_2 - L_3^2}X_{e_f}^2 + \frac{\alpha}{2}\Delta\theta^2 =$$

$$\frac{1}{2}\tilde{x}^T Q_0\tilde{x} + L_3\tilde{i}_f\tilde{i}_q\Delta\theta + \frac{1}{L_1(L_1L_2 - L_3^2)}(L_3\tilde{X}_{e_d} - L_1\tilde{X}_{e_f})^2 +$$

$$\frac{1}{L_1}\tilde{X}_{e_q}^2 + \frac{1}{L_1 L_2 - L_3^2}X_{e_f}^2 + \frac{\alpha}{2}\Delta\theta^2 \tag{5.25}$$

where $\tilde{X}_e = X_e - X_{e_s} = \begin{bmatrix} \tilde{X}_{e_d} \\ \tilde{X}_{e_q} \\ \tilde{X}_f \end{bmatrix}$ and $\tilde{i} = \begin{bmatrix} \tilde{i}_d \\ \tilde{i}_q \\ \tilde{i}_f \end{bmatrix}$.

Then the desired overall Hamiltonian function satisfies,

$$H_d(\tilde{x}(t)) = H_d(\tilde{x}(0)) - \int_0^t \nabla H^T(\tilde{x}(s)) R_d(\tilde{x}(t)) \nabla H_d(\tilde{x}(s)) ds$$

We seek a state feedback control law $u_f(\tilde{x})$ and $u_p(\tilde{x})$, so that

$$H(u_f(\tilde{x}), u_p(\tilde{x})) = H_d \tag{5.26}$$

Proposition 5.5.1. The system given in (5.22Control Designequation.5.5.22), with the state feedback controller:

$$u_f = u_{f_s} + \frac{2}{3}(\frac{L_3}{L_1})(R_1 + \omega_r L_1 \Delta\theta)\left(3\tilde{i}_d + 2\frac{L_3}{L_1}\tilde{i}_f\right) + \frac{1}{3}(\frac{L_3}{L_1})(2R_1\Delta\theta + \omega_r L_1)\left(3\tilde{i}_q + 2\frac{L_3}{L_1}\Delta\theta\tilde{i}_f\right) \tag{5.27}$$

and

$$u_p = 2v_{d_s}\tilde{i}_d + 2v_{q_s}\tilde{i}_q + 2\frac{L_3}{L_1}\tilde{i}_f(v_{d_s} + \Delta\theta v_{q_s}) - \alpha\Delta\theta \tag{5.28}$$

with the gain $\alpha \geq 0$ results in the following closed loop system:

$$\dot{\tilde{x}} = (J_d(\tilde{x}) - R_d(\tilde{x}))\nabla H_d(\tilde{x}) \tag{5.29}$$

where

$$J_d(\tilde{x}) = \begin{bmatrix} J_{line} & I & B' \\ -I & J_{load} & 0 \\ -B'^T & 0 & J_{d_{inv}} \end{bmatrix},$$

$$R_d(\tilde{x}) = diag(R_{line}, R_{load}, R_{d_{inv}})$$

$$J_{d_{inv}}(\tilde{x}) = \begin{bmatrix} 0 & -a & b & -v_{d_s} & 0 \\ a & 0 & c & -v_{q_s} & 0 \\ -b & -c & 0 & -u_{f_s} & 0 \\ v_{d_s} & v_{q_s} & u_{f_s} & 0 & -1 \\ 0 & 0 & 0 & 1 & 0 \end{bmatrix}$$

and

$$R_{d_{inv}}(\tilde{x}) = \begin{bmatrix} \frac{R_1}{3} & 0 & 0 & 0 & 0 \\ 0 & \frac{R_1}{3} & 0 & 0 & 0 \\ 0 & 0 & R_2 & 0 & 0 \\ 0 & 0 & 0 & d & 0 \\ 0 & 0 & 0 & 0 & 0 \end{bmatrix}$$

where $a = \frac{\omega_r L_1}{3}$, $b = \frac{2}{3}(\frac{L_3}{L_1})(R_1 + \omega_r L_1 \Delta\theta)$, $c = \frac{1}{3}(\frac{L_3}{L_1})(2R_1\Delta\theta + \omega_r L_1)$ and x_s is an equilibrium of the above system.

Proof Substituting (5.27equation.5.5.27) and (5.28equation.5.5.28) into (5.22Control Designequation.5.5.22) gives (5.29equation.5.5.29) after some manipulations.

Proposition 5.5.2. The closed-loop system (5.29equation.5.5.29) has a unique equilibrium point at $\tilde{x}_* = 0$.

Proof At the equilibrium point of (5.29equation.5.5.29),

$$(J_d - R_d)\nabla H_d(\tilde{x}_*) = 0 \tag{5.30}$$

Note that,

$$det(J_d - R_d) =$$

$$(\frac{L_3}{L_1})^2(\frac{R_2}{27})\left(4(R_1 + \omega_r L_1 \Delta\theta)^2 + (2R_1\Delta\theta + \omega_r L_1)^2\right)$$

Consequently, the matrix $J_d - R_d$ is nonsingular for all nonzero values of R_2 and L_3 and thus (5.26Control Designequation.5.5.26) requires

$$\nabla H_d(\tilde{x}_*) = 0$$

We know that $\nabla H_{line}|_{x=x_s} = 0$, $\nabla H_{load}|_{x=x_s} = 0$ and for the inverter-based generator we must have,

$$\nabla H_{d_{inv}}|_{x=x_s} = \begin{bmatrix} 3\tilde{i}_d + 2(\frac{L_3}{L_1})\tilde{i}_f \\ 3\tilde{i}_q + 2(\frac{L_3}{L_1})\Delta\theta\tilde{i}_f \\ \tilde{i}_f \\ \Delta\omega \\ -\tilde{i}_f\tilde{i}_q L_3 + \alpha\Delta\theta \end{bmatrix} = 0 \tag{5.31}$$

Consequently, $\tilde{i}_f = 0$, $\tilde{i}_d = 0$, $\tilde{i}_q = 0$, $\Delta\omega = 0$ and $\Delta\theta = 0$ thus $\tilde{x}_* = 0$.

5.6 Stability

In this section we discuss the stability of the open loop microgrid system as well as the closed loop system with controller (5.27equation.5.5.27)-(5.28equation.5.5.28). We start with the uncontrolled system.

Proposition 5.6.1. Considering system (5.22Control Designequation.5.5.22) with constant control $\tilde{u} = 0$ then for any fixed value of $\Delta\theta$, system (5.22Control Designequation.5.5.22) has an equilibrium point. At equilibrium point $\Delta\dot{\theta} = \Delta\omega_* = 0$ so $\Delta\theta(t) = \Delta\theta(0)$.
For $L_1 \geq 0$ and $L_1 L_2 \geq L_3^2$, if $|\Delta\theta| \leq \frac{\sqrt{L_1 L_2 - L_3^2}}{|L_3|}$, we have $Q(\Delta\theta) \geq 0$ and thus $H(\tilde{x})$ is a positive semi-definite function i.e. $H(\tilde{x}) \geq 0$. Furthermore, if $R_1 R2 \geq (\frac{\omega_r L_3}{2})^2$ the open loop system is stable.

Proof The open-loop dissipation matrix is, $\tilde{R} = diag(R_{line}, R_{load}, R_{inv})$, where R_{line}, R_{load} and R_{inv} represent line, load and inverter-based generator dissipation matrices, respectively. For $R_1 R_2 \geq (\frac{\omega_r L_3}{2})^2$, the matrix $\tilde{R}$ is positive semi-definite i.e. $\tilde{R} \geq 0$. The time-derivative of H_d is,

$$\dot{H}(\tilde{x}) = -\nabla H(\tilde{x}) R \nabla H(\tilde{x}) \leq 0 \tag{5.32}$$

so $\dot{H}_d(\tilde{x}) \leq 0$ and consequently the system is stable.

We apply the Lyapunov theorem in the analysis of the stability of the closed loop system (5.29equation.5.5.29) at the desired equilibrium point. In the port-Hamiltonian formulation of the system the best candidate for Lyapunov function is frequently the Hamiltonian function. In the remainder of this section we investigate

conditions for stability of the controlled system via Lyapunov stability and the properties of the port-Hamiltonian representation of the system.

The added terms in H_d are a function of inverter-based generator states,

$$H_d(\tilde{x}) = H(\tilde{x}) + G(\tilde{x}_{inv})$$

where $\tilde{x}_{inv}$ are the states associated to the inverter-based generator. Note that we have,

$$\nabla H_d = col(\nabla H_{line}, \nabla H_{load}, \nabla H_{d_{inv}})$$

Proposition 5.6.2. For parameter values $L_1 \geq 0$, $L_1L_2 - L_3^2 \geq 0$, $\frac{L_3}{L_1} \leq 1$, $L_1L_2 \leq 2.5L_3$ and $L_1L_2 - L_3^2 = L_3$, the closed-loop system with the state feedback law in proposition 5.5.1prop.5.5.1 is globally asymptotically stable.

Proof By proposition 5.5.2prop.5.5.2, the closed loop Hamiltonian function has an isolated minimum at the desired equilibrium point i.e. $\nabla H_d|_{x=x_s} = 0$. First we will show that under stated conditions the energy function H_d in (5.25Control Designequation.5.5.25) is positive definite. We have,

$$\tilde{X}_{e_d} = L_1\tilde{i}_d + L_3\tilde{i}_f \tag{5.33}$$

and

$$\tilde{X_{e_f}} = L_3\tilde{i}_d + L_3\Delta\theta\tilde{i}_q + L_2\tilde{i}_f$$

Consequently,

$$L_3\tilde{X}_{e_d} - L_1\tilde{X}_{e_f} = (L_3^2 - L_1L_2)\tilde{i}_f - L_3L_1\Delta\theta\tilde{i}_q$$

and the first term in (5.25Control Designequation.5.5.25) is,

$$\frac{1}{2}\tilde{x}^T Q_0 \tilde{x} = \frac{1}{2}(L_1\tilde{i}_d^2 + 2L_3\tilde{i}_d\tilde{i}_q + L_1\tilde{i}_q^2 + L_2\tilde{i}_f^2)$$

$$= \frac{L_1}{2}(\tilde{i}_d + \alpha\tilde{i}_q)^2 + \frac{L_1}{2}(1-\alpha^2)\tilde{i}_q^2 + \frac{L_2}{2}\tilde{i}_f^2 \tag{5.34}$$

Let $\alpha = \frac{L_3}{L_1} \leq 1$ and note that $\frac{L_3}{L_1 L_2 - L_3^2} = 1$. Then, the second term in (5.25Control Designequation.5.5.25) becomes,

$$\frac{1}{L_1(L_1L_2 - L_3^2)}(L_3\tilde{X}_{e_d} - L_1\tilde{X}_{e_f})^2$$

$$= \frac{1}{L_1 L_3}\left[(L_3^2 - L_1L_2)\tilde{i}_f - L_1L_3\Delta\theta\tilde{i}_q\right]^2$$

$$= \frac{L_3}{L_1}(\tilde{i}_f^2 + L_1^2\Delta\theta^2\tilde{i}_q^2 + 2L_1\Delta\theta\tilde{i}_f\tilde{i}_q) \tag{5.35}$$

Now we add (5.34Stabilityequation.5.6.34) and $L_3\tilde{i}_f\tilde{i}_q\Delta\theta$ to (5.35Stabilityequation.5.6.35),

$$(\frac{L_3}{L_1} + \frac{L_2}{2})\tilde{i}_f^2 + L_3L_1\Delta\theta^2\tilde{i}_q^2 + 3L_3\Delta\theta\tilde{i}_f\tilde{i}_q \tag{5.36}$$

that is positive if,

$$2\sqrt{(\frac{L_3}{L_1} + \frac{L_2}{2})}\sqrt{(L_3L_1)} \leq 3L_3 \tag{5.37}$$

then,

$$L_1L_2 \leq 2.5L_3$$

The rest of terms in (5.25Control Designequation.5.5.25) are non-negative. This shows that $H_d(\tilde{x})$ is a positive definite function with $H_d(0) = 0$.

The time derivative of the closed loop Hamiltonian function H_d is non-positive. Indeed,

$$\dot{H}_d = \nabla H_d^T\dot{\tilde{x}} = -\nabla H_d^T R_d \nabla H_d$$

R_d is positive-semi definite so $\dot{H}_d \leq 0$. The state values where $\dot{H}_d = 0$ are points of the from $(0, 0, ..., 0, \Delta\theta)$. Since $\Delta\omega = 0$ we have $\Delta\theta = \Delta\theta_0$ and by Lasalle's principle the system is asymptotically stable.

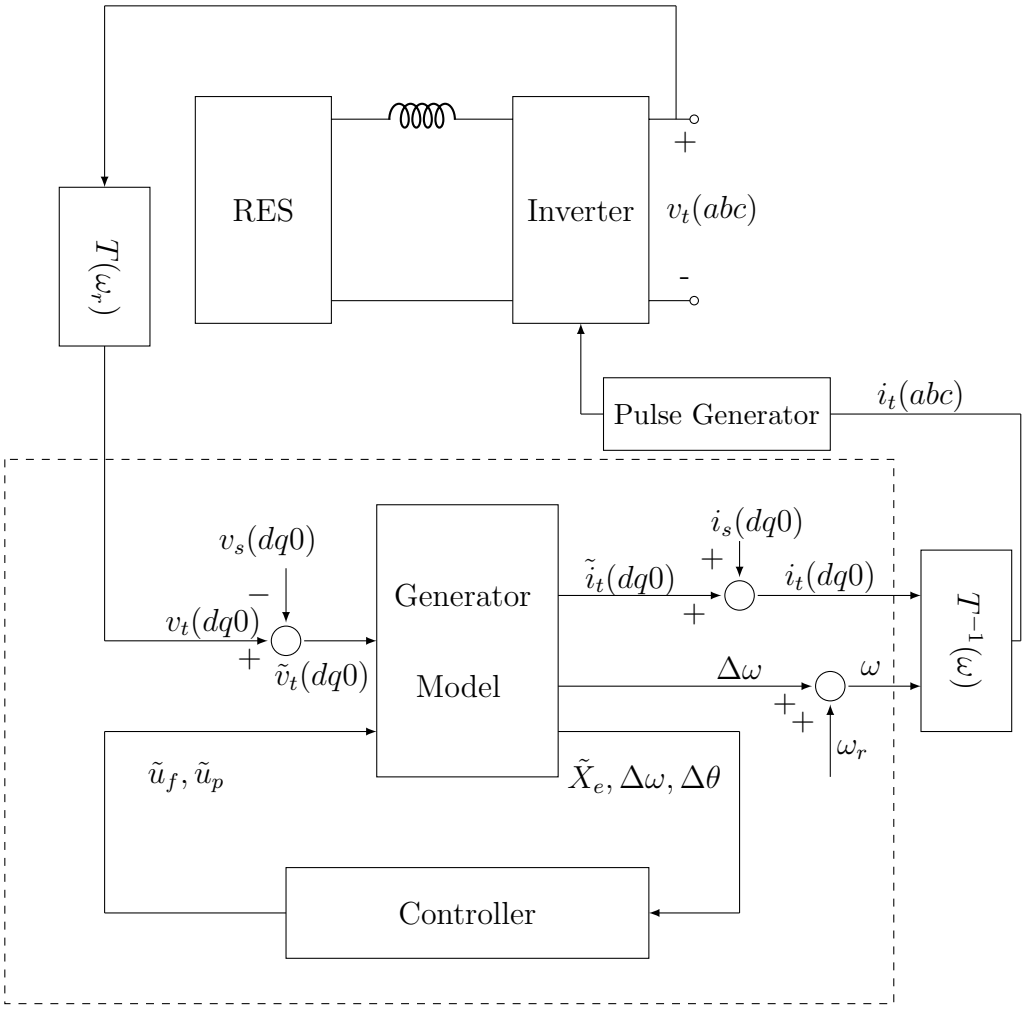

Figure 5.7: Schematic diagram of the closed-loop inverter-based controller.

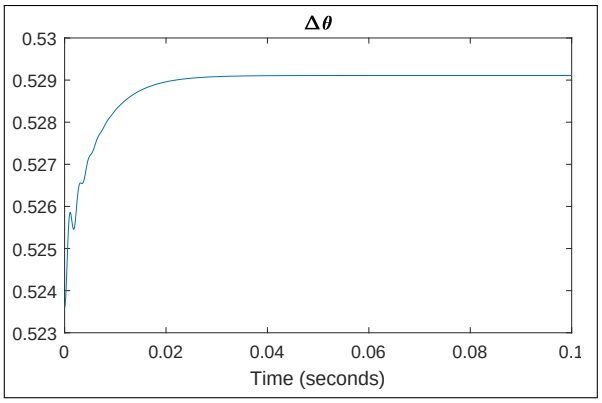

Figure 5.8: $\Delta\theta$ in open loop system for initial value $\frac{\pi}{6}$

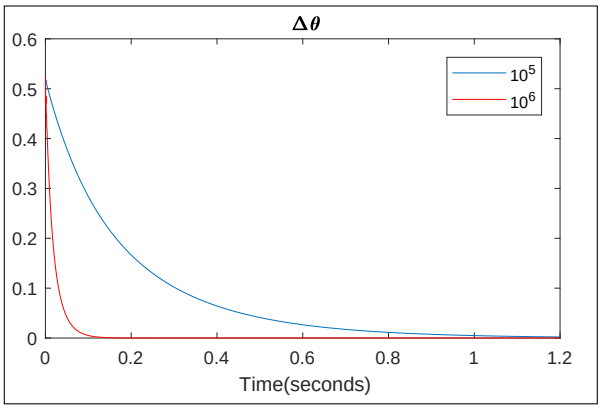

Figure 5.9: $\Delta\theta$ for different values of α in the closed-loop system ($\alpha = 10^6$).

5.7 Example

We developed a simulation platform to examine the port-Hamiltonian model of system consisting of a constant impedance load, a π line and an inverter-based generator.

First we examined the performance of the open loop inverter-based generator with a constant input $\tilde{u}_p = 0$ and $\tilde{u}_f = 0$. The system is open loop stable with the selected values of parameters but as Fig. 5.8$\Delta\theta$ in open loop system for initial value $\frac{\pi}{6}$figure.5.8 show $\Delta\theta(t)$ does not converge to zero.

The performance of the closed loop system was evaluated for different values of

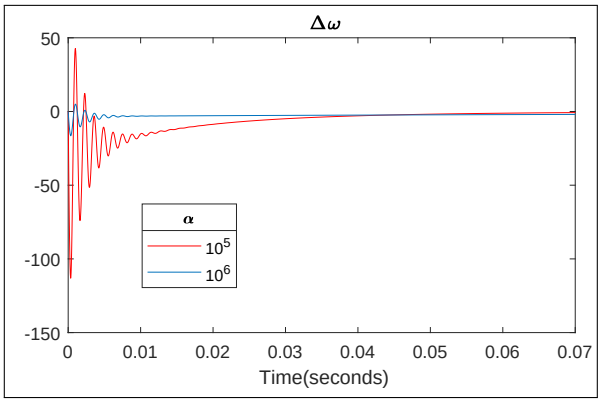

Figure 5.10: $\Delta\omega$ for different values of α in the closed-loop system ($\alpha = 10^6$).

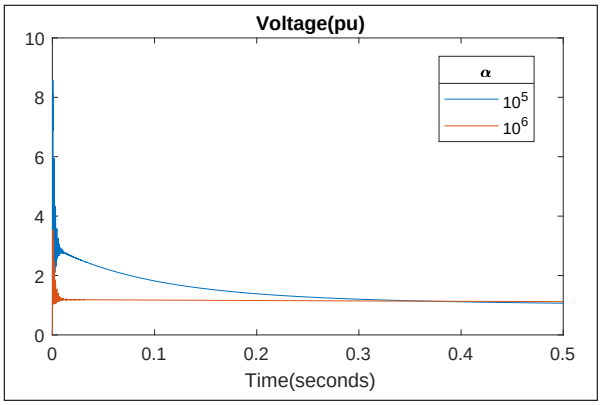

Figure 5.11: Inverter-based generator terminal voltage for different values of α in the closed-loop system

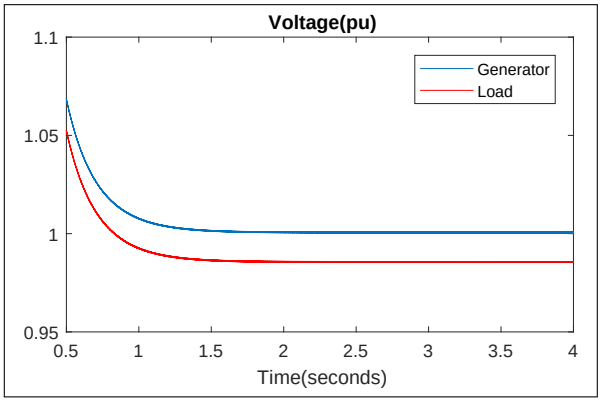

Figure 5.12: Generator and load terminal voltage.

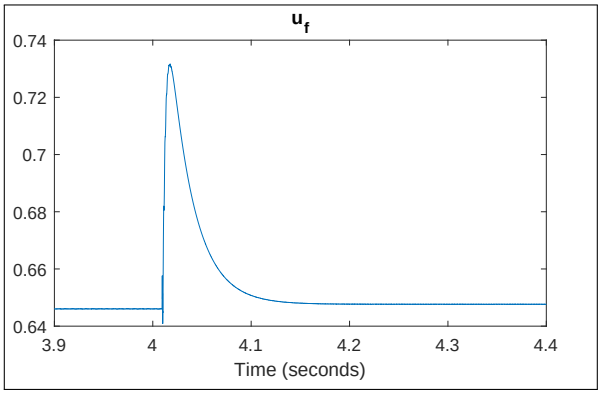

Figure 5.13: $\tilde{u}_f$ when a 50 percent increase in load resistance occurs($\alpha = 10^6$).

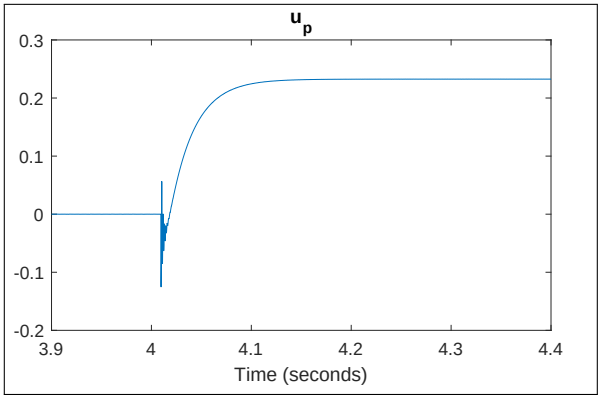

Figure 5.14: $\tilde{u}_p$ when a 50 percent increase in load resistance occurs($\alpha = 10^6$).

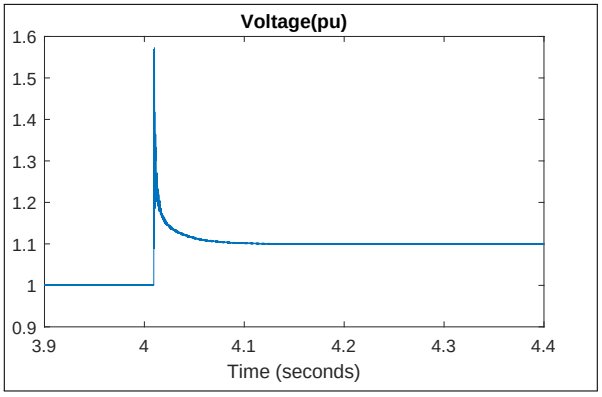

Figure 5.15: Inverter-based generator terminal voltage when a 50 percent increase in load resistance occurs($\alpha = 10^6$).

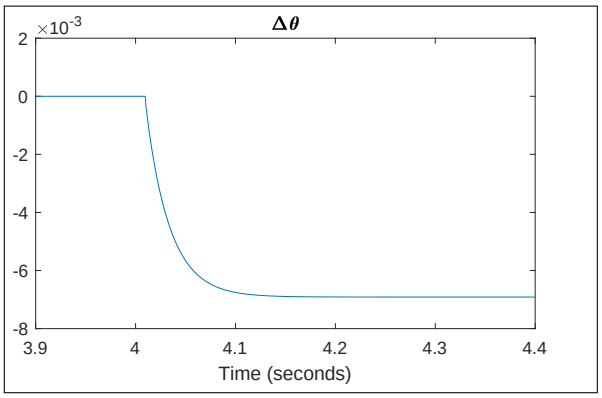

Figure 5.16: Phase angle when a 50 percent increase in load resistance occurs($\alpha = 10^6$).

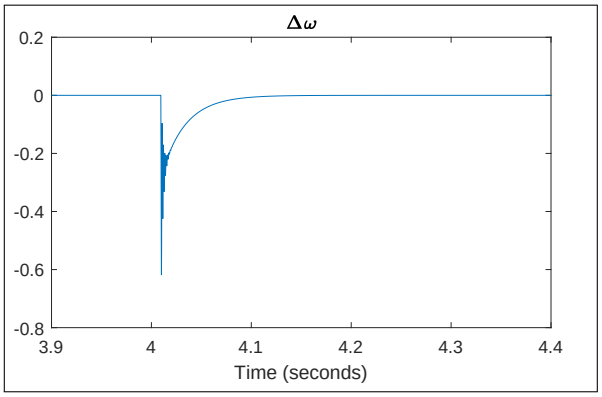

Figure 5.17: Frequency deviation when a 50 percent increase in load resistance occurs($\alpha = 10^6$).

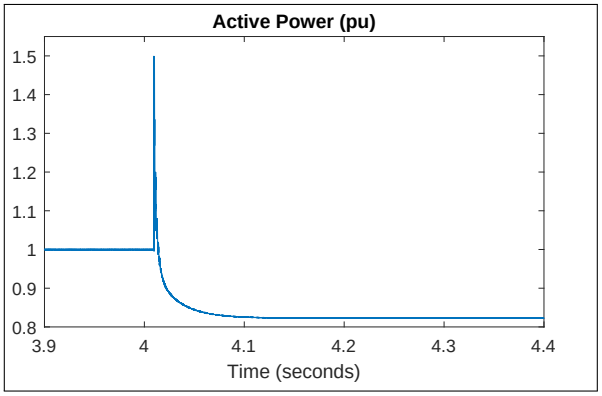

Figure 5.18: Active power when a 50 percent increase in load resistance occurs($\alpha = 10^6$).

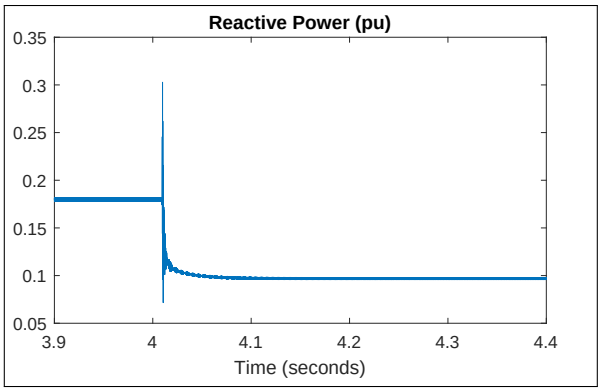

Figure 5.19: Reactive power when a 50 percent increase in load resistance occurs($\alpha = 10^6$).

the tuning parameter α. Fig. 5.9$\Delta\theta$ for different values of α in the closed-loop system ($\alpha = 10^6$)figure.5.9 shows that $\Delta\theta$ converges to zero but convergence rate depends critically on the controller parameter α as shows in Fig. 5.10$\Delta\omega$ for different values of α in the closed-loop system ($\alpha = 10^6$)figure.5.10. Furthermore, the convergence rate and dynamics of $\Delta\omega$ depend critically on α. Finally, Fig. 5.11Inverter-based generator terminal voltage for different values of α in the closed-loop systemfigure.5.11 shows that the generator terminal voltage convergence rate critically depends on α. Fig. 5.12Generator and load terminal voltagefigure.5.12 shows the performance of the generator and load voltages for a fixed value of $\alpha = 10^6$.

The performance of the controlled system was evaluated as function of a step change in the load. i.e. the load resistance was changed by 50% (power factor from 93.58 % to 96.99%). Fig. 5.13$\tilde{u}_f$ when a 50 percent increase in load resistance occurs($\alpha = 10^6$)figure.5.13 and 5.14$\tilde{u}_p$ when a 50 percent increase in load resistance occurs($\alpha = 10^6$)figure.5.14 show the response of the two control variables to the load change. Fig. 5.15Inverter-based generator terminal voltage when a 50 percent increase in load resistance occurs($\alpha = 10^6$)figure.5.15 and 5.16Phase angle

when a 50 percent increase in load resistance occurs($\alpha = 10^6$)figure.5.16 show that the terminal voltage and the state $\Delta\theta$ converged to the new steady state values as function of the load change while the steady state value of the frequency did not change as is shown in Fig. 5.17Frequency deviation when a 50 percent increase in load resistance occurs($\alpha = 10^6$)figure.5.17, Fig. 5.18Active power when a 50 percent increase in load resistance occurs($\alpha = 10^6$)figure.5.18 and 5.19Reactive power when a 50 percent increase in load resistance occurs($\alpha = 10^6$)figure.5.19 show that the real and reactive powers converge quickly to their new values.

5.8 Summary

In this chapter we have presented a VSM approach for the control of an inverter-based generator. The developed approach is based on a full dynamical port-Hamiltonian formulation that emulates synchronous generator behavior. The approach is developed for both CSI and VSI type of inverters. The results are demonstrated in a simple example of a generator connected to a simple microgrid.

Chapter 6

Conclusion

Modern power systems have components that have power electronic interfaces that are both fast and can have complex controlled behavior at the interfaces. Consequently, time scale separation that is often used in the analysis of power system dynamics may no longer be valid and traditional load models are not sufficient. The development of a new modeling and analysis paradigm that does not depend on time scale separation and is general enough to facilitate the modeling of complex loads and generators with power electronics is needed.

To provide simplicity in operating inverter-based generation units, there are various control strategies based on emulating the critical properties of a conventional synchronous generator such as inertia and damping. This dissertation designs a novel operational and control model for controlled power electronic loads and inverter-based generators inspired by synchronous generators' equations and stated in port-Hamiltonian systems' formulation. Within the context of Port-Hamiltonian power system formulation we developed:

- Virtual Synchronous Machine (VSM) control architecture for both Current Source Inverter (CSI) and Voltage Source Inverter (VSI).
- General load model that incorporate complex loads such as Constant Power Loads.

Bibliography

[1] E. Allen, N. LaWhite, Y. Yoon, J. Chapman, and M. Ilic, "Interactive object-oriented simulation of interconnected power systems using simulink," *IEEE Transactions on Education*, vol. 44, no. 1, pp. 87–94, Feb 2001.

[2] E. H. Allen and M. D. Ilic, "Interaction of transmission network and load phasor dynamics in electric power systems," *IEEE Transactions on Circuits and Systems I: Fundamental Theory and Applications*, vol. 47, no. 11, pp. 1613–1620, Nov 2000.

[3] H. A. Alsiraji and R. El-Shatshat, "Comprehensive assessment of virtual synchronous machine based voltage source converter controllers," *IET Generation, Transmission Distribution*, vol. 11, no. 7, pp. 1762–1769, 2017.

[4] S. M. Ashabani and Y. A. I. Mohamed, "A flexible control strategy for grid-connected and islanded microgrids with enhanced stability using nonlinear microgrid stabilizer," *IEEE Transactions on Smart Grid*, vol. 3, no. 3, pp. 1291–1301, Sept 2012.

[5] E. Barklund, N. Pogaku, M. Prodanovic, C. Hernandez-Aramburo, and T. C. Green, "Energy management in autonomous microgrid using stability-constrained droop control of inverters," *IEEE Transactions on Power Electronics*, vol. 23, no. 5, pp. 2346–2352, Sept 2008.

[6] H. Beck and R. Hesse, "Virtual synchronous machine," pp. 1–6, Oct 2007.

[7] M. Belkhayat, R. Cooley, and A. Witulski, "Large signal stability criteria for distributed systems with constant power loads," in *Proceedings of PESC '95 - Power Electronics Specialist Conference*, vol. 2, June 1995, pp. 1333–1338 vol.2.

[8] Y. Chen, R. Hesse, D. Turschner, and H. Beck, "Dynamic properties of the virtual synchronous machine (visma)," *Renewable Energy and Power Quality Journal*, 05 2011.

[9] ——, "Improving the grid power quality using virtual synchronous machines," pp. 1–6, May 2011.

[10] ——, "Comparison of methods for implementing virtual synchronous machine on inverters," *Int. Conf. on Renewable Energies and Power Quality*, pp. 1–6, 2012.

[11] J. Chow, J. Winkelman, M. Pai, and P. Sauer, "Singular perturbation analysis of large-scale power systems," *International Journal of Electrical Power Energy Systems*, vol. 12, no. 2, pp. 117 – 126, 1990. [Online]. Available: http://www.sciencedirect.com/science/article/pii/014206159090007X

[12] S. D'Arco and J. A. Suul, "Virtual synchronous machines classification of implementations and analysis of equivalence to droop controllers for microgrids," pp. 1–7, June 2013.

[13] ——, "Equivalence of virtual synchronous machines and frequency droops for converter based microgrids," *IEEE Transactions on Smart Grid*, vol. 5, no. 1, pp. 394–395, Jan 2014.

[14] P. Dondi, D. Bayoumi, C. Haederli, D. Julian, and M. Suter, "Network integration of distributed power generation," *Journal of Power Sources*, vol. 106, no. 1, pp. 1 – 9, 2002, proceedings of the Seventh Grove Fuel Cell Symposium. [Online]. Available: http://www.sciencedirect.com/science/article/pii/S037877530101031X

[15] S. Fiaz, D. Zonetti, R. Ortega, J. Scherpen, and A. van der Schaft, "A port-hamiltonian approach to power network modeling and analysis," *European Journal of Control*, vol. 19, no. 6, pp. 477 – 485, 2013. [Online]. Available: http://www.sciencedirect.com/science/article/pii/S094735801300157X

[16] M. Galaz, R. Ortega, A. S. Bazanella, and A. M. Stankovic, "An energy-shaping approach to the design of excitation control of synchronous generators," *Automatica*, vol. 39, no. 1, pp. 111 – 119, 2003. [Online]. Available: http://www.sciencedirect.com/science/article/pii/S0005109802001772

[17] B. Ge, A. N. Ghule, and D. C. Ludois, "A dq-axis framework for electrostatic synchronous machines and charge oriented control," pp. 2396–2403, Oct 2017.

[18] J. Grainger and w.D. Stevenson, "Power system analysis," in *McGraw-Hill, Inc, New York*, 1994.

[19] T. Green and M. Prodanovi, "Control of inverter-based micro-grids," *Electric Power Systems Research*, vol. 77, no. 9, pp.

1204 – 1213, 2007, distributed Generation. [Online]. Available: http://www.sciencedirect.com/science/article/pii/S037877960600191X

[20] D. J. Hill, "Nonlinear dynamic load models with recovery for voltage stability studies," *IEEE Transactions on Power Systems*, vol. 8, no. 1, pp. 166–176, Feb 1993.

[21] M. A. Hossain, H. R. Pota, W. Issa, and M. J. Hossain, "Overview of ac microgrid controls with inverter-interfaced generations," *Energies*, vol. 10, no. 9, 2017.

[22] J. Iannacci, "Rf-mems for high-performance and widely reconfigurable passive components a review with focus on future telecommunications, internet of things (iot) and 5g applications," *Journal of King Saud University - Science*, vol. 29, no. 4, pp. 436 – 443, 2017, sI: Smart materials applications of new materials. [Online]. Available: http://www.sciencedirect.com/science/article/pii/S1018364717304007

[23] C. L. M. J. A. Peas Lopes, "Defining control strategies for microgrids islanded operation," *IEEE Transactions on Power Systems*, vol. 21, no. 2, May 2006.

[24] J. B. J. Machowski, J.W. Bialek, "Power system dynamics stability and control," *Wiley*, 2008, 2nd ed.

[25] Z. Jankovic, B. Novakovic, V. Bhavaraju, and A. Nasiri, "Average modeling of a three-phase inverter for integration in a microgrid," pp. 793–799, Sept 2014.

[26] F. Katiraei, R. Iravani, N. Hatziargyriou, and A. Dimeas, "Microgrids management," *IEEE Power and Energy Magazine*, vol. 6, no. 3, pp. 54–65, May 2008.

[27] H. K. Khalil, "Output feedback control of linear two time scale systems," pp. 1397–1400, June 1985.

[28] D. A. Koester, K. W. Markus, and M. D. Walters, "Mems: small machines for the microelectronics age," *Computer*, vol. 29, no. 1, pp. 93–94, Jan 1996.

[29] P. Kokotovi, H. Khalil, and J. O'Reilly, *Singular Perturbation Methods in Control: Analysis and Design.* Society for Industrial and Applied Mathematics, 1999. [Online]. Available: https://epubs.siam.org/doi/abs/10.1137/1.9781611971118

[30] A. Kumar and D. Chatterjee, "A survey on space vector pulse width modulation technique for a two-level inverter," pp. 78–83, Dec 2017.

[31] S. Kundu and I. A. Hiskens, "Overvoltages due to synchronous tripping of plug-in electric-vehicle chargers following voltage dips," *IEEE Transactions on Power Delivery*, vol. 29, no. 3, pp. 1147–1156, June 2014.

[32] B. Lasseter, "Microgrids [distributed power generation]," vol. 1, pp. 146–149 vol.1, Jan 2001.

[33] R. H. Lasseter, "Microgrids," vol. 1, pp. 305–308 vol.1, Jan 2002.

[34] M. W. Layland, "Generalised electrostatic-machine theory," *Proceedings of the Institution of Electrical Engineers*, vol. 116, no. 3, pp. 403–405, March 1969.

[35] Y. Li, D. M. Vilathgamuwa, and P. C. Loh, "Design, analysis, and real-time testing of a controller for multibus microgrid system," *IEEE Transactions on Power Electronics*, vol. 19, no. 5, pp. 1195–1204, Sept 2004.

[36] Y. A. I. Mohamed and E. F. El-Saadany, "Adaptive decentralized droop controller to preserve power sharing stability of paralleled inverters in distributed generation microgrids," *IEEE Transactions on Power Electronics*, vol. 23, no. 6, pp. 2806–2816, Nov 2008.

[37] A. Mohd, E. Ortjohann, D. Morton, and O. Omari, "Review of control techniques for inverters parallel operation," *Electric Power Systems Research*, vol. 80, no. 12, pp. 1477 – 1487, 2010. [Online]. Available: http://www.sciencedirect.com/science/article/pii/S0378779610001392

[38] I. J. Nagrath and D. P. Kothari, *Modern power system analysis*. New Delhi : Tata McGraw-Hill, 1980.

[39] D. E. Olivares, A. Mehrizi-Sani, A. H. Etemadi, C. A. Caizares, R. Iravani, M. Kazerani, A. H. Hajimiragha, O. Gomis-Bellmunt, M. Saeedifard, R. Palma-Behnke, G. A. Jimnez-Estvez, and N. D. Hatziargyriou, "Trends in microgrid control," *IEEE Transactions on Smart Grid*, vol. 5, no. 4, pp. 1905–1919, July 2014.

[40] R. Ortega, A. J. V. D. Schaft, I. Mareels, and B. Maschke, "Putting energy back in control," *IEEE Control Systems Magazine*, vol. 21, no. 2, pp. 18–33, April 2001.

[41] R. Ortega, A. van der Schaft, F. Castanos, A. Astolfi, and A. Astolfi, "Control by interconnection and standard passivity-based control of port-hamiltonian systems," *IEEE Transactions on Automatic Control*, vol. 53, no. 11, pp. 2527–2542, Dec 2008.

[42] R. Ortega, A. van der Schaft, B. Maschke, and G. Escobar, "Interconnection and damping assignment passivity-based control of port-controlled hamiltonian systems," *Automatica*, vol. 38, no. 4, pp. 585 – 596, 2002. [Online]. Available: http://www.sciencedirect.com/science/article/pii/S0005109801002783

[43] M. K. Pal, "Voltage stability conditions considering load characteristics," *IEEE Transactions on Power Systems*, vol. 7, no. 1, pp. 243–249, Feb 1992.

[44] O. Pizniur, "Active adaptive auxiliary circuit for stabilizing dc distribution systems with constant power loads," Ph.D. dissertation, University of British Columbia, 2015. [Online]. Available: https://open.library.ubc.ca/collections/ubctheses/24/items/1.0166216

[45] Z. Qu, S. Ebrahimi, N. Amiri, and J. Jatskevich, "Stabilizing integrated power systems with constant-power loads based on dc bus voltage monitoring," pp. 155–159, Aug 2018.

[46] A. Riccobono and E. Santi, "Comprehensive review of stability criteria for dc power distribution systems," *IEEE Transactions on Industry Applications*, vol. 50, no. 5, pp. 3525–3535, Sept 2014.

[47] T. Runolfsson, "On the dynamics of three phase electrical energy systems," pp. 6827–6832, July 2016.

[48] K. Sakimoto, Y. Miura, and T. Ise, "Stabilization of a power system with a distributed generator by a virtual synchronous generator function," pp. 1498–1505, May 2011.

[49] G. Santosuosso, "Passivity of nonlinear systems with input-output feedthrough," *Automatica*, vol. 33, no. 4, pp. 693 – 697, 1997. [Online]. Available: http://www.sciencedirect.com/science/article/pii/S0005109896002002

[50] S. Sastry, "Nonlinear systems: Analysis, stability and control," in *Springer-Verlag*, 1999.

[51] J. Schiffer, R. Ortega, A. Astolfi, J. Raisch, and T. Sezi, "Conditions for stability of droop controlled inverter based microgrids," *Automatica*, vol. 50, no. 10, pp. 2457 – 2469, 2014. [Online]. Available: http://www.sciencedirect.com/science/article/pii/S0005109814003100

[52] J. G. Slootweg and W. L. Kling, "Impacts of distributed generation on power system transient stability," vol. 2, pp. 862–867 vol.2, July 2002.

[53] S. D. Sudhoff, K. A. Corzine, S. F. Glover, H. J. Hegner, and H. N. Robey, "Dc link stabilized field oriented control of electric propulsion systems," *IEEE Transactions on Energy Conversion*, vol. 13, no. 1, pp. 27–33, March 1998.

[54] U. B. Tayab, M. A. B. Roslan, L. J. Hwai, and M. Kashif, "A review of droop control techniques for microgrid," *Renewable and Sustainable Energy Reviews*, vol. 76, pp. 717 – 727, 2017. [Online]. Available: http://www.sciencedirect.com/science/article/pii/S1364032117303453

[55] A. van der Schaft, *L2-Gain and Passivity Techniques in Nonlinear Control*, 3rd ed. Springer Publishing Company, Incorporated, 2016.

[56] J. C. Willems, "Paradigms and puzzles in the theory of dynamical systems," *IEEE Transactions on Automatic Control*, vol. 36, no. 3, pp. 259–294, March 1991.

[57] Q. Zhong and G. Weiss, "Static synchronous generators for distributed generation and renewable energy," in *2009 IEEE/PES Power Systems Conference and Exposition*, March 2009, pp. 1–6.

[58] ——, "Synchronverters: Inverters that mimic synchronous generators," *IEEE Transactions on Industrial Electronics*, vol. 58, no. 4, pp. 1259–1267, April 2011.